Stratigraphy and morphogenesis of Pleistocene coral reefs at Tambolaka (Sumba Island, Indonesia)

Gino De Gelder[1,2*], Tubagus Solihuddin[1*], Dwi Amanda Utami[1], Marfasran Hendrizan[1], Rima Rachmayani[3], Denovan Chauveau[4], Christine Authemayou[5], Laurent Husson[2], Sri Yudawati Cahyarini[1]

[1]Paleoclimate & Paleoenvironment Research Group, National Research and Innovation Agency (BRIN), Bandung, Indonesia

[2]ISTerre, CNRS, IRD, Univ. Grenoble Alpes, Grenoble, France

[3]Oceanography Research Group, Faculty of Earth Sciences and Technology, Bandung Institute of Technology, Indonesia

[4]Dipartimento di Scienze Ambientali, Informatica e Statistica (DAIS), Ca' Foscari University of Venice, Venice, Italy

[5]LGO, IUEM, CNRS, UMR 6538, Université de Bretagne Occidentale, Plouzané, France

* Both authors contributed equally to this paper and share first-authorship

Abstract

The fossil record of Quaternary reef systems, as expressed in uplifted regions by sequences of stacked terraces, has been extensively used to either understand their morphodynamics, or to unravel sea level variations. Yet, because these two aspects are intimately linked, Quaternary reef analysis is often underdetermined because the analysis often focuses on single sequences, along one-dimensional profiles. Here, we take advantage of the lateral variations of coral reef sequences by documenting the morphological variations of the reef sequence on Sumba Island. Near Tambolaka, Northwest Sumba, we analyzed a reef transect, topography, and associated sedimentological record to obtain a precise coral reef stratigraphy and geomorphic patterns that can be compared to the well documented eastern counterpart. In Tambolaka, the reef sequence displays four lower layers of bedded chalky limestone units with a weakly cemented sandy matrix, which we attribute to the Middle Miocene to Pliocene Wakabukak formation based on calcareous nannofossils and planktonic foraminifers. The uppermost layer is a calcretized reefal limestone unit with a well-lithified sandy matrix, which we attribute to the Plio-Pleistocene reef sequence of the Kalianga formation. Seven marine terraces imprint the regional morphology, four of which we correlate with MIS 5e, MIS 7e, MIS 9e, MIS 11c terraces of Cape Laundi, Northeast Sumba. When scrutinized at the light of numerical models of reef development, these results indicate that the morphodynamics of reefal sequences is strongly impacted by the tectonic evolution, even at local scales. The geodynamic context sets both the extrinsic -morphology of the basement, hydrodynamics- conditions of reef development, but also the intrinsic properties -reef growth rate in particular. While the morphodynamic evolution of the sequence is at first order representative of the interplay between uplift rates and sea level oscillations, the detailed assemblage of the reef units drastically varies along the coastline.

Keywords: Coral reefs, Marine Terraces, Uplift, Sea-level, Tectonics, Northwest Sumba

1. INTRODUCTION

Studies of coral reef terrace sequences provide crucial clues about past sea levels and tectonic activity (e.g. Chappell, 1974; Taylor and Mann, 1991; Bard et al., 1996). As living coral reefs adjust to relative sea-level variations, their fossilized counterparts act as geomorphic and biological markers of past relative sea levels. Due to their extent, preservation, and datable material, some coral reef terrace sequences have received much more attention, than others, like Barbados (Fairbanks, 1989; Peltier and Fairbanks, 2006), Huon in Papua New Guinea (Chappell and Polach, 1991; De Gelder et al., 2022) and Sumba in Indonesia (Pirazzoli et al., 1991, 1993; Bard et al., 1996). In all of these locations, most studies have been dedicated to a few key profiles: the reef sections in Barbados (Fairbanks, 1989; Peltier and Fairbanks, 2006), the Bobongora, Kanzarua, and Sialum sections in Huon (Chappell and Polach, 1991; De Gelder et al., 2022) and the Cape Laundi section in Sumba (Pirazzoli et al., 1991, 1993; Hantoro et al., 1992; Chauveau et al., 2021a).

Numerical geomorphic analysis of high-resolution digital elevation models together with numerical models of coral reef growth have provided a breakthrough in understanding the links between sea level changes and the morphological record of coastlines. Especially for Huon, it has been demonstrated that it is worthwhile to consider the lateral variations in terrace elevations, ages, and uplift rates, to better constrain paleo sea-level and tectonic processes (De Gelder et al., 2022). On Sumba Island, although several studies have pointed out the lateral changes in terrace elevations (Nexer et al., 2015; Authemayou et al., 2018; 2022), little is known about the coral reef terraces outside of the Cape Laundi profile. In this study, we aim to fill that gap, by exploring geologic and geomorphic lateral variations between Cape Laundi, and the coral reef terraces ~100 km westward.

Sumba Island is part of the Lesser Sunda Islands Group comprising mainly the islands of Bali-Lombok-Sumbawa-Flores-Alor-Wetar. The island is interpreted as a micro-continent from Sundaland that moved to its current position ~20 Ma (Early Miocene), when the islands group of Lesser Sunda had not yet been formed (Hamilton, 1979; Burollet & Salle, 1981; Soeria-Atmadja et al., 1998; Abdullah et al., 2000; Satyana & Purwaningsih, 2011a). The regional tectonic setting has determined much of the contemporary landforms and controlled the development of the uplifted landscapes by which Quaternary reef systems have emerged (Jouannic et al., 1988; Pirazzoli et al., 1991, 1993; Bard et al., 1996).

Quaternary reefs in Sumba Island have developed over the Tertiary (Mio-Pliocene) limestones of the Waikabubak Formation in the western part and marly sandstones of the Kananggar Formation in the eastern part, forming major geomorphic features for over 300 km across the island. While the reef systems in NE Sumba have been well-studied, especially at Cape Laundi (Pirazzoli et al., 1991, 1993; Chauveau et al., 2021a, 2021b), the reef systems in NW Sumba are relatively poorly recognized and understudied. Yet, the morphology of the Quaternary reefs profoundly varies along-strike, and it is still unclear how the well-identified geomorphic patterns from the Quaternary reefs of E Sumba correlate to the coral reef sequence of W Sumba, or how they have developed as distinctive morphologies driven by different tectonic settings.

A comprehensive study from Nexer et al. (2015) demonstrated morphometric indices of catchment areas across the Quaternary reefal limestone of Sumba Island to derive coastal uplift rates based on analysis of a single highstand of Cape Laundi marine terraces IIIb, which they correlated with the Marine Isotope Stage (MIS) 11. More recently, Chauveau et al., 2021a revisited the chronology of the Cape Laundi sequence through an integrated approach combining ^{36}Cl cosmogenic concentrations and $^{230}Th/U$ ages. Chauveau et al., 2021b

characterized the dynamics of coastal drainage in Cape Laundi based on high-resolution topographic data, geomorphological analysis, and denudation rates derived from ^{36}Cl cosmogenic nuclide concentrations. Authemayou et al. (2018) underlined the role of normal faults as the main driving force in the drainage rearrangement of W-Sumba in addition to asymmetric uplift and groundwater flow. Authemayou et al. (2022) used structural data, marine terrace analysis, drainage evolution and focal mechanisms around Sumba to show that the island is affected by dextral en-echelon folding triggered by subduction of the western lateral boundary of the Australian continental margin. However, no comprehensive chronological framework has been proposed in a previous study for the NW-Sumba coral reef terraces.

This study focuses on a reef transect to assess the reef lithostratigraphy within the exposed mine pit of Tambolaka, NW-Sumba. The outcrop enables detailed stratigraphic, paleoecological, and geochronological analyses spanning the entire reef growth history. Furthermore, we present a detailed geologic/geomorphic comparison between Tambolaka in NW-Sumba and Cape Laundi in NE-Sumba, using a combination of geomorphic indices and numerical reef modeling. This integration allows us to address features like reef geochronology, accretion history, and uplift rates of NW-Sumba. Thus, the primary aim of this paper is to obtain 1) a better understanding of reef lithostratigraphy in NW-Sumba through a reef transect within the exposed mine pit of Tambolaka, 2) lateral variations including terrace elevations, ages, and uplift rates between Cape Laundi NE-Sumba and Tambolaka NW-Sumba through a detailed analysis of changes in geomorphology, and 3) geomorphic patterns and potential growth of reef sequences in W Sumba through numerical reef modeling. Since geometry, composition, and evolution of coral reef systems provide important geological estimates of past relative sea levels and tectonic motions (Camoin & Webster, 2015), this paper provides a basic framework for considering past and future modes of reef response to sea level and tectonic changes at various time scales.

2. BACKGROUND

2.1 Geological Setting

Sumba Island is part of the Wallacea region, a transitional area between Asiatic fauna groups in the west and Australia in the east, characterized by a high level of endemicity and local specific faunas (Satyana & Purwaningsih, 2011b). Based on rock characteristics, fossil composition, and gravity analysis, it is thought that Sumba Island was probably once part of Sundaland, and drifted southwards by back-arc spreading from South Sulawesi to its current position in the Early Miocene (Rangin et al., 1990; Wensik and Van Bergen, 1995; Rutherford et al., 2001; Hall, 2002; Hall and Smyth, 2008; Satyana and Purwaningsih, 2011a). During the Late Miocene, thick buoyant continental Australian crust subducted under the Banda arc, causing the Sumba ridge to rise and emerge (Harris, 1991; Fortuin et al., 1997; Hall and Smyth, 2008; Haig, 2012; Tate et al., 2014). This rise resulted in 1) the diachronic emergence of Sumba ridge 3 Ma years ago in the east and 1 Ma years ago at Cape Laundi (Pirazzoli et al., 1993), 2) the formation of Quaternary coral reef terraces on the northern flank, and 3) a coeval south-verging collapse of the southern flank (Fleury et al., 2009; Authemayou et al., 2018).

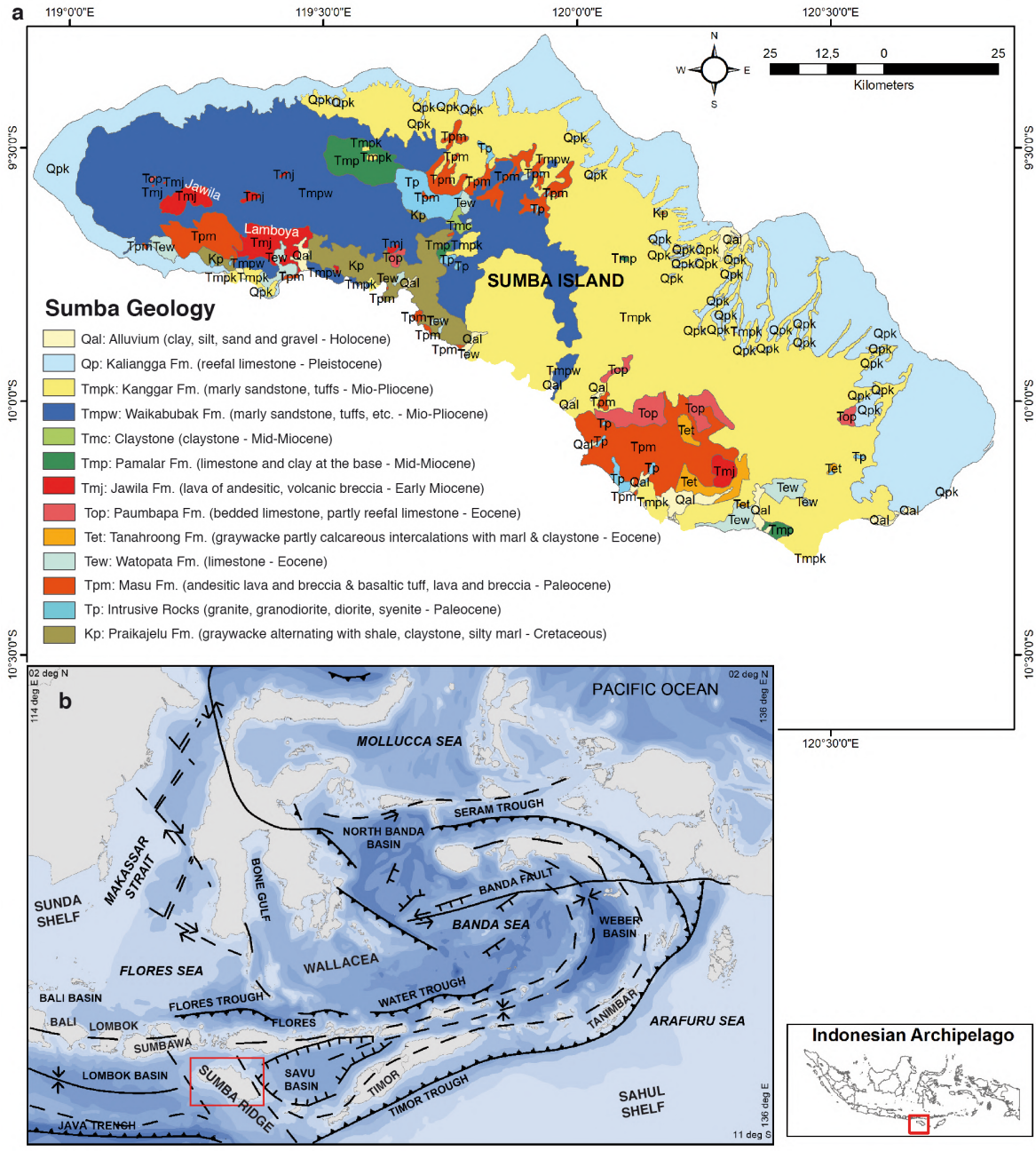

Figure 1. Geological map and tectonic setting of Sumba Island. (a) *Geological map of Sumba Island (after Effendi & Apandi, 1993)* ***(b)*** *Sumba Island in the regional tectonic setting of Eastern Indonesia (after Hamilton, 1979; Burollet and Salle, 1981; Abdullah et al., 2000).*

Sumba Island tectonically lies at the plate boundary and transitions from oceanic subduction in the west to island arc-continent collision in the east. To the west, the oceanic crust of the Indo-Australian plate subducts beneath the Sunda arc at the Java Trench (Figure 1). To the east, conversely, the Australian continental crust underthrusts the Banda arc at the Timor Trough since the Late Miocene. This event remodeled subduction dynamics, and profoundly reshaped the entire morphotectonic pattern of the region, as it triggered the pervasive subsidence of the Sunda Shelf in the West and the Sahul Shelf in the Southeast, while uplifting Wallacea in between (Husson et al., 2023), and the islands Flores, Timor and Sumba in particular (e.g. Miller et al., 2021), where it formed a collision zone

(Pacheco et al., 1993; Hall, 2002, 2012; Bock et al., 2003; Nugroho et al., 2009; Spakman and Hall, 2010; Simons et al., 2007; Harris, 2011; Satyana and Purwaningsih, 2011a; Authemayou et al., 2022). Consequently, two trench systems border southern Sumba Island (Satyana & Purwaningsih, 2011b). First, the 6 km deep Java Trench -associated with the Sunda Arc- is located south of Bali and Sumbawa, where the oceanic lithosphere of the Indo-Australian plate subducts below Sundaland. Second, the 3 km deep Timor trough stretches from the south of Sumba Island towards the northeast, where the continental lithosphere of the Indo-Australian plate subducts beneath Timor, Tanimbar and some smaller islands (Figure 1; Satyana & Purwaningsih, 2011b). The subduction of the Indo-Australian plate in the Sunda Trench has formed the active volcanic islands of Bali, Lombok, Sumbawa, Flores, and some smaller islands.

2.2 Stratigraphy

The oldest rock exposed on Sumba Island (Figure 1) on the southern coast of Sumba is the Praikajelu Formation. This formation is composed of Late Cretaceous greywacke, shale, clay, stone, silty marl, and clayey sandstone. During the Paleocene, two significant magmatic periods formed the lavas and andesitic breccias of the Masu Formation and intrusive rocks (granite, granodiorite, diorite, syenite). Overlying these are the Eocene limestones of the Watopata Formation interfingering with the partly calcareous greywacke of Tanahroong Formation. Following this, the Paumbapa Formation consists of partly reefal limestones that were unconformably deposited during the Oligocene. The mid-Miocene claystones of the Pamalar Formation and were deposited in an unconformity (Effendi & Apandi, 1993).

On the western side, the Mio-Pliocene rocks are composed of widespread transgressive carbonate series of the Waikabubak Formation consisting of limestones, clayey limestones, and tuffaceous marls. On the eastern side, the turbiditic chalky sediments of Kananggar Formation consist of marly sandstones, tuffaceous sandstones, tuffs, sandy marls, and limestones. The Neogene was marked by syn-sedimentary tectonics, evidenced by normal faulting and large-scale slumping (Authemayou et al., 2018). The Quaternary rocks are reefal limestones of the Kaliangga Formation overlay the Waikabubak and Kananggar Formations. Recent alluviums are composed of clays, silts, sands, and gravels (Effendi & Apandi, 1993; Astjario, 2006).

3. METHODOLOGY AND METHODS

3.1 Mapping

The land topography data covering the study area are derived from a DEMNAS Digital Elevation Model (http://tides.big.go.id/DEMNAS) with a spatial resolution of 0.27 arc-seconds of longitude and latitude (an arc-second of longitude and latitude equals 30.87 m at the equator) and referenced to the Earth Gravitational Model (EGM) 2008 for the vertical datum. The DEM combines elevation data from IFSAR and TERRASAR-X with a spatial resolution of 5 m, respectively, and ALOS PALSAR with a spatial resolution of 11.25 m, in addition to the mass point data resulting from stereo-plotting. The ocean topography was extracted from BATNAS (https://tanahair.indonesia.go.id/demnas/#/batnas). This bathymetric data was acquired using a field survey from the Center for Marine and Coastal Environment, the Geospatial Information Agency of the Republic of Indonesia. It has largely been generated from a database with interpolation between soundings guided by satellite-derived gravity data. The spatial resolution of BATNAS data is

6 arc-seconds of latitude and longitude according to the MSL datum. The extracted elevation data were exported into points in ASCII format which were then used to generate a bathymetric grid using a Triangulated Irregular Network (TIN) method within the Global Mapper v16.0 toolkit.

We used these elevation data to systematically map the sequence of the reef terraces on slope maps and elevation maps. The landward limit of Quaternary reefal terraces on the large-scale map (Figure 2a) was based on the morphologic contrast in roughness between the relatively smooth Quaternary terraces, and relatively high-relief older formations, and corroborated with the geological map (Figure 1). The seaward limit of the Quaternary reefal terraces was approximated by the 130 m bathymetric isobath. This number approximately corresponds to the sea-level depth during the Last Glacial Maximum (~20 ka), which should be indicative of the lowermost limit of Quaternary terraces in uplifting areas like Sumba. The reef terrace mapping of the Cape Laundi terraces is based on Chauveau et al. (2021a), whereas the reef mapping of the Tambolaka section is based on a lateral correlation of reef terraces and morphological observations.

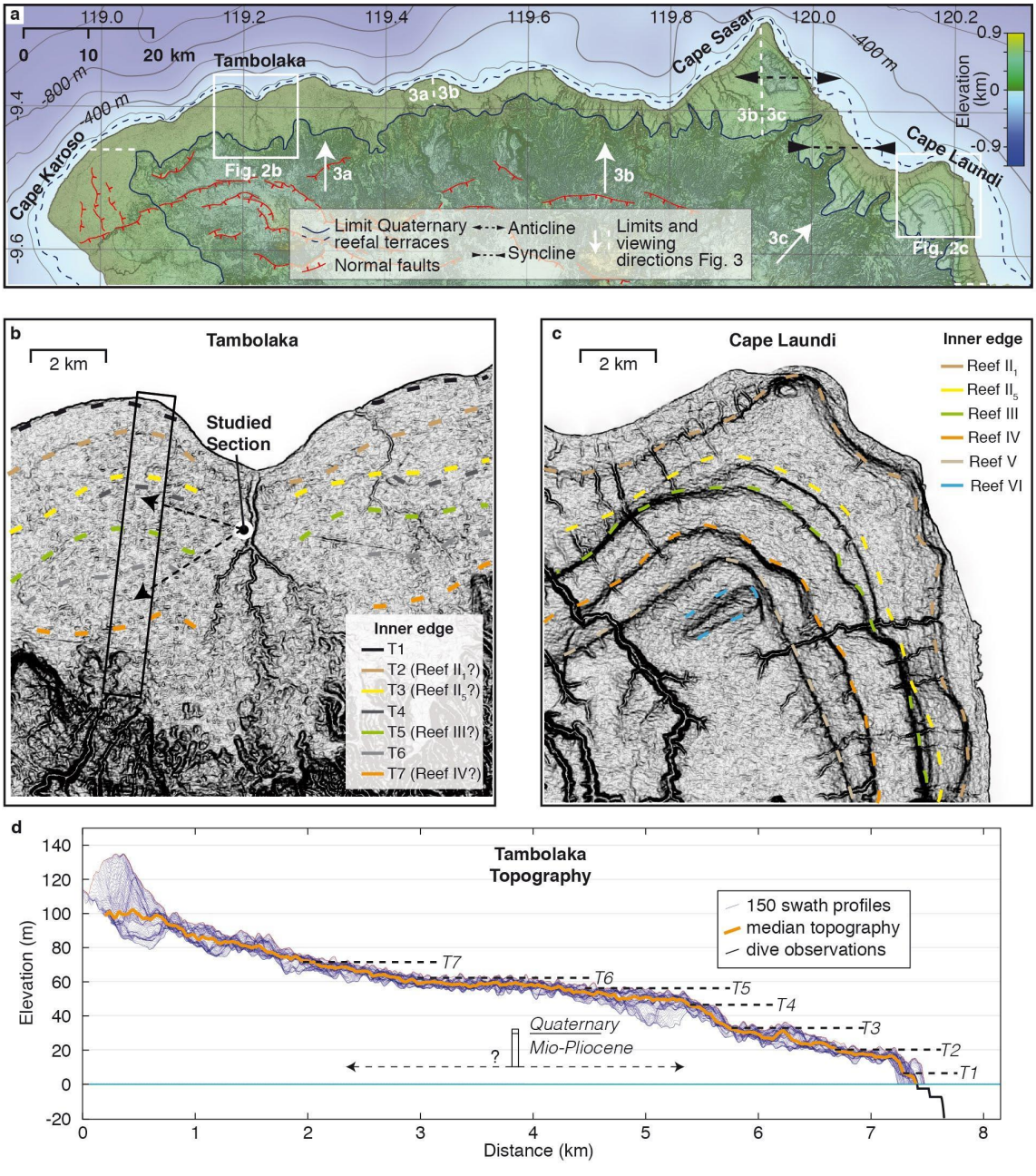

Figure 2. Coral reef terraces between Cape Laundi and Tambolaka (a) *Slope map of the NW-Sumba coastal area studied here, overlain with colored elevations. Limits of Quaternary reefal terraces were drawn from the BATNAS bathymetry and DEMNAS topography (see materials and methods), whereas normal faults and folds are re-drawn from Authemayou et al. (2022)* ***(b)*** *Slope map of the Tambolaka area, with the location of the stratigraphic section analyzed here and 7 mapped coral reef terrace levels* ***(c)*** *Slope map of Cape Laundi area, with reef labels and inner edges from Chauveau et al. (2021a)* ***(d)*** *Stacked swath profile of the Tambolaka coral reef terrace sequence, with its location given in* ***b****, and bathymetric observations made by diving in the shallow reef areas offshore. Below the stacked swath profile, we show the possible location of our stratigraphic section when translated from its location near the river to this cross-section.*

3.2 Stratigraphic log and fossil analysis

A reef transect was established to log the sedimentary exposures in the Tambolaka open-cut pit and the transect line was selected along with the workable exposure. Using DEMNAS DEM, we estimated the base of the pit at 8 ± 2 m above sea level (masl). A vertical transect from the base to the top (~23 m high, so between 8 and 31 masl) was logged, sampled, and photographed to obtain information including 1) the ratio of coral clasts and matrix (following Embry and Klovan, 1971); 2) sediment textural characteristics (using the Udden-Wentworth nomenclature and a visual assessment of sediment composition); 3) preliminary coral generic identification. Reef framework analysis and facies descriptions follow Montaggioni (2005), which highlights the growth forms of the dominant coral reef builders and key environmental indicators. Position fixing uses a built-in GPS and camera on a smartphone.

Rock samples for fossil analysis were collected from a subset of transects on every reef sequence. At each sampling site, 1 kg of rock samples was collected for planktonic foraminifera identification as necessary. All samples were washed through a 63 μm sieve and dried at 40°C temperature overnight. The residue from a gram of samples was examined using the binocular microscope Olympus SZX40 and the portable scanning electron microscope (SEM) Phenom ProX Thermo 4th generation at the Research Center for Climate and Atmosphere of BRIN. Foraminifera and calcareous nannofossils are identified based on a previous study by Bolli et al. (1985).

3.3 Geomorphological analysis

To have a detailed understanding of lateral variability in geomorphic characteristics of the N-Sumba coast, we assessed coral reef terrace elevations, present-day reef widths, offshore reefal terrace widths, and offshore slopes between Cape Laundi and Tambolaka. To assess coral reef terrace elevations, we used stacked swaths (Armijo et al., 2015; Fernández-Blanco et al., 2020), which is a combined plot of hundreds of parallel topographic profiles that can aid in understanding lateral coral reef terrace correlations (De Gelder et al., 2022). To obtain a good balance between readability and detail, we opted for 900 parallel profiles of 20 m width, using average elevation measurements for every 50 m along the profile. For the area between Tambolaka and Cape Sasar, we used an Northward viewing angle (Figure 2a), and for the area between Cape Sasar and Cape Laundi a NE-ward viewing angle (N041E; Figure 2a), in both cases roughly parallel to the present-day coastline. We limited this analysis to the topography of onshore Quaternary reefal terraces. For the lateral correlation of reef elevations, we used the same reef nomenclature as in Chauveau et al. (2022) at Cape Laundi

and assessed the continuity of the terraces W-ward for the inner edges of 4 reefs (Reefs II_1, II_5, III, and IV), both using the stacked swath profiles and in map view. We selected these reef units as reference datum, as ages (Pirazzoli et al., 1993; Bard et al., 1996) and modeling (Chauveau et al., 2022) suggest that they emerged during the 4 most recent major interglacial highstands: MIS 5e (~125 ka), MIS 7e (~240 ka), MIS 9e (~325 ka) and MIS 11c (~400 ka). As sea-level elevations during these highstands were relatively high, the corresponding terraces can be expected to be currently exposed above sea level even for relatively low uplift rates (Pastier et al., 2019; De Gelder et al., 2022).

To calculate the present-day reef width, we used historical imagery from Google Earth, marking the reef edge roughly every 150 m along the coastline, wherever it was clearly visible from the imagery. We did the same for the present-day coastline and used linear interpolation for both the present-day coastline and reef edge to have measurements exactly every 150 m. As for the stacked swaths, we used an N-S orientation to calculate the reef width between Tambolaka and Cape Sasar and a NE-SW (N041E) orientation for the reef between Cape Sasar and Cape Laundi. We corrected for the local orientation of the coastline to approximate the width perpendicular to the coastline, using the following equation for the interval between Tambolaka and Cape Sasar:

$$PRW_i = ORW_i \cdot \cos(\tan^{-1} \frac{|y_{i-1} - y_{i+1}|}{|x_{i-1} - x_{i+1}|}) \quad \text{(Eq. 1)}$$

in which PRW is the perpendicular reef width, ORW the oblique reef width, y_{i-1} and x_{i-1} the coordinates in UTM m for the measurement 150 m to the west, and y_{i+1} and x_{i+1} for the measurement 150 m to the east. For the section between Cape Sasar and Cape Laundi we applied the same equation, but after rotating both the coastline and reef edge by 41° counterclockwise. For all the resulting reef width estimates we applied a 5-km moving average to filter out short wavelength variations in relation to small river outlets.

To calculate the offshore reefal terrace width, we used the same procedure as Equation 1 but measured the difference between the present-day coastline and the -130 m depth contour (Figure 2a) instead. To calculate the offshore slope as a percentage, we also used the same procedure as Equation 1 but estimated the horizontal distance between the -130 m and -200 m contour (Figure 2a), and the horizontal distance between the -130 and -400 m contour (Figure 2a) instead. We then divided 70 and 270 m, respectively, by those distances.

3.4 Reef Modeling

Landscape evolution models provide a way to evaluate the full geometry of a marine terrace sequence, not just the elevation of a terrace, and help distinguish the most likely chronology (De Gelder et al., 2020). To reproduce the coral reef terrace sequence at Tambolaka and evaluate to what extent the controlling parameters vary between Cape Laundi and Tambolaka, we use the REEF code (see details in Husson et al., 2018; Pastier et al., 2019). This model provides a way to simulate the geomorphic response that can be expected given different initial slopes, uplift rates, reef growth rates, eroded volumes, and sea-level histories.

We selected a topographic profile ~2 km West of the Tambolaka River (Figure 2b), which may have caused anomalous sedimentation and erosion patterns during the development of the reefal sequence -at short distances from the stream- but also remodeled the landscape during subaerial exposure following uplift. The slope of this profile is between 1% and 2%, which we both tested as input parameters. We tested uplift rates of 0.125, 0.15, and 0.175 mm/yr, as the reef elevations at Tambolaka are approximately between 1/3rd and 1/4th of the

elevations at Cape Laundi, which are thought to be uplifting at rates of ~0.5 mm/yr (Chauveau et al., 2022). We used potential reef growth rates between 1 and 6 mm/yr, the former being the minimum value in the REEF model, and the latter the best-fitting reef growth rate for Cape Laundi (Chauveau et al., 2022). For eroded volumes, we tested 60 mm^3/yr (as in Chauveau et al., 2022), as well as higher values of 180 and 360 mm^3/yr given the generally stronger waves and currents in Tambolaka compared to Cape Laundi. We ran the models for 1 Ma and tested 4 different sea-level curves that were derived with different methodologies: 1) the sea-level curve of Waelbroeck et al. (2002) derived from a composite $\delta^{18}O$ curve that was corrected with a global coral data compilation, 2) the curve of Bintanja et al. (2005) derived through inverse ice-sheet modeling, 3) the curve of Grant et al. (2014) derived by hydraulic models in the Red Sea Basin, and 4) the curve of Spratt and Lisiecki (2016) derived from a principal component analysis of 7 other sea-level curves. The only one of these curves spanning 1 Ma is the curve of Bintanja et al. (2005), so we added the sea-level elevations of Bintanja et al. (2005) for the intervals that are absent in the other curves: 450-1000 ka for Waelbroeck et al. (2002), 500-1000 ka for Grant et al. (2014), and 800-1000 ka for Spratt and Lisiecki (2016).

4. RESULTS

4.1 Stratigraphy and paleoecology

Stratigraphic and paleoecological data from the measured reef section of Tambolaka can be summarized as follows (Figure 3); the lowermost section of the open-cut pit is a bedded chalky limestone unit (up to ~7 m thick) with a sandy matrix. The rock mainly contains recrystallized corals and a weakly cemented, pale yellow, fine to coarse grain-sized sandy matrix. This unit mainly consists of domal corals with a diameter no larger than 30 cm. Faviidae are predominant including *Cyphastrea, Platygyra, Diploastrea, Uolophyllia*, and *Leptastrea spp.* (Figure 4). Overlying this, a two-bedded chalky limestone unit (~5 m thick each) contains crystalline arborescent and domal coral fragments in a weakly cemented, pale gray, fine to coarse-grained sandy matrix. Coral colonies are generally small, hardly identified, and invariably recrystallized. Above this unit is a brownish-chalky limestone (up to ~5 m thick) with a fine to coarse-grained sandy matrix. Coral colonies are dominated by Poritidae including *Goniopora* and *Porites spp.* but also contain colonies from the genera of Merulinidae such as *Hydnophora sp* (Figure 4). Coral colonies are typically small, approximately 10 – 30 cm in diameter. All stratigraphic sections of the bedded chalky limestone are matrix-supported and classified as floatstone reef facies with abundant and diverse molluscan fauna.

A calcretized reefal limestone unit of 1 to 1.5 m of thickness is present in the uppermost portion of the reef sequences in the measured section profile. This is a minimum thickness because the top of this unit is eroded, and it may thus be thicker elsewhere (Figure 3). The rock primarily contains coralline algae with minor coral. Coral fragments are mostly crystallized in a well-cemented, dark gray, fine to coarse-grained sandy matrix. Shell fragments, sea urchins, and gastropods are abundant. The coral clasts are visually well-coated with encrusted algae.

The measured section of the Tambolaka mine pit contains rare and well-preserved foraminifera and calcareous nannofossil assemblages. Planktonic foraminifera in this limestone unit consists of *Globorotalia opima opima, Globorotalia tumida, Globorotalia pertenuis, Globorotalia pseudomiocenica,* and *Globorotalia plesiotumida* (Figure 5). These foraminifera assemblages indicate a

wide age range between the Oligocene and Pliocene. Besides foraminifera, calcareous nannofossils are identified in a bedded chalky limestone unit at the bottom of the unit (Figure 6). Several genera of calcareous nannofossil identified in that layer are *Calcidiscus, Helicosphaera, Coccolithus, Discoaster, Umbilicosphaera,* and *Reticulofenestra.* The relative ages of the strata, based on analysis of calcareous nannofossils, range from Middle Miocene to Pliocene in the lowermost bedded chalky limestone, based on the presence of both *Umbilicosphaera sibogae* (Middle Miocene-Pleistocene) and *Calcidiscus macintirey* (Early Miocene-Pliocene) in the same assemblage (Fig. 6). One species of *Discoaster mohleri* was found in the fossil reef deposit of the Tambolaka mine pit, suggesting a Paleocene age. However, we believe this nannofossil has been reworked from an older formation.

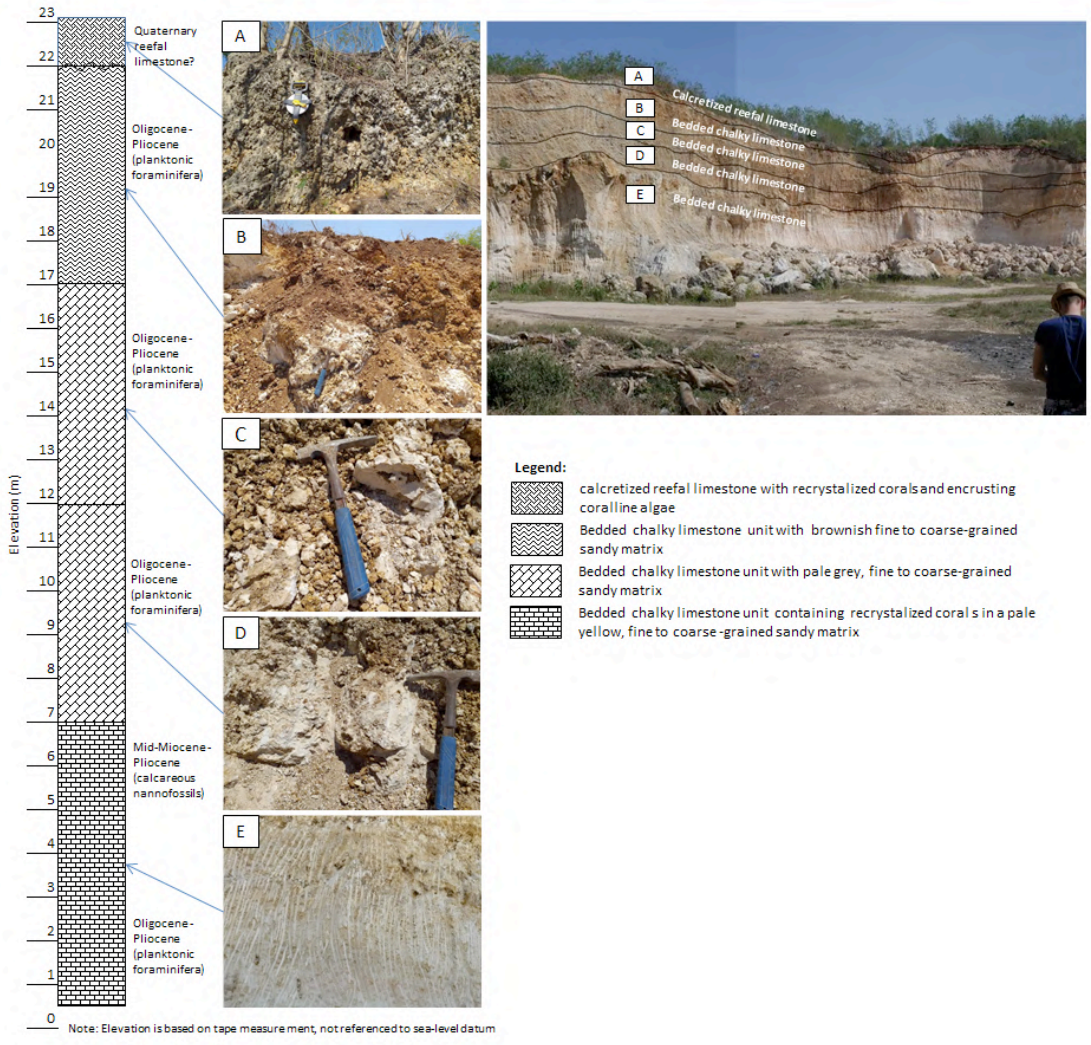

Figure 3. Lithostratigraphic summary of the measured reef section. *Section of Tambolaka mine-pit showing at least five different reef assemblages.*

Based on the fossil record, we conclude that the sequence is mostly Middle Miocene to Pliocene in age, which we assign to the Waikabukak formation (Figure 1). The lithology indicates that the Pleistocene to recent Kalianga formation there is only represented by the topmost unit, that clearly display the typical facies of a fossil coral reef unit.

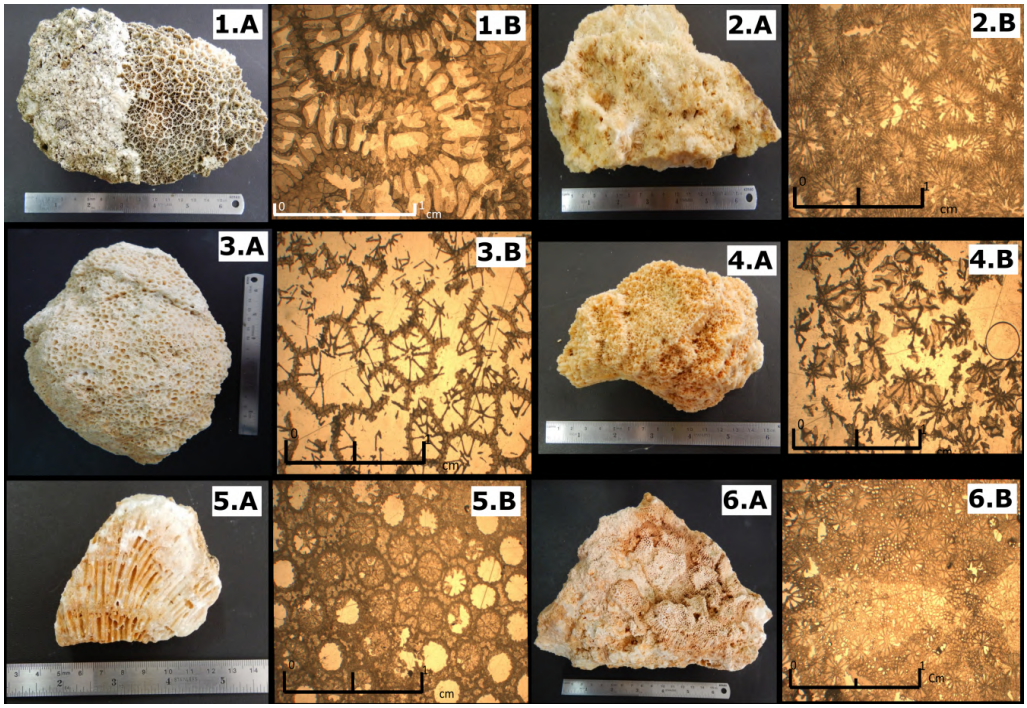

Figure 4. Coral colonies of the bedded chalky limestone units of the Tambolaka mine pit. *Corals were identified from the lowermost layer and the fourth layer of the measured reef sequences. Letter A indicates coral colonies and B shows thin sections of the coral colonies. The coral colonies are 1. Platygyra sp, 2. Diploastrea sp, 3. Leptastrea sp, 4. Hydnophora sp, 5. Goniopora sp, and 6. Porites sp.*

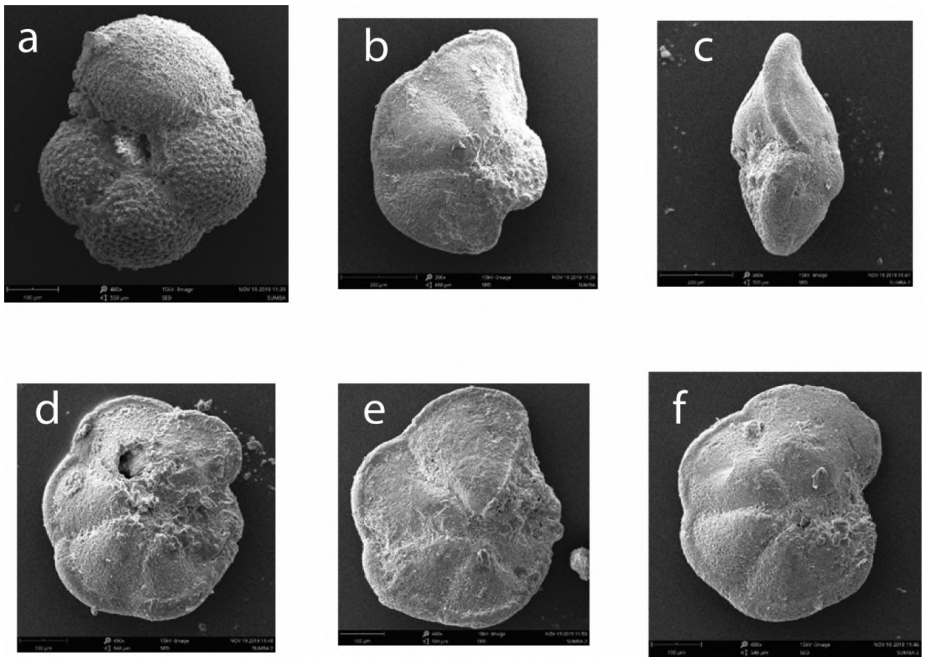

Figure 5. Planktonic Foraminifera assemblages in a bedded chalky unit. ***(a)*** *Globorotalia opima opima* ***(b)*** *Globorotalia tumida* ***(c)*** *Globorotalia tumida* ***(d)*** *Globorotalia pertenuis* ***(e)*** *Globorotalia pseudomiocenica* ***(f)*** *Globorotalia plesiotumida.*

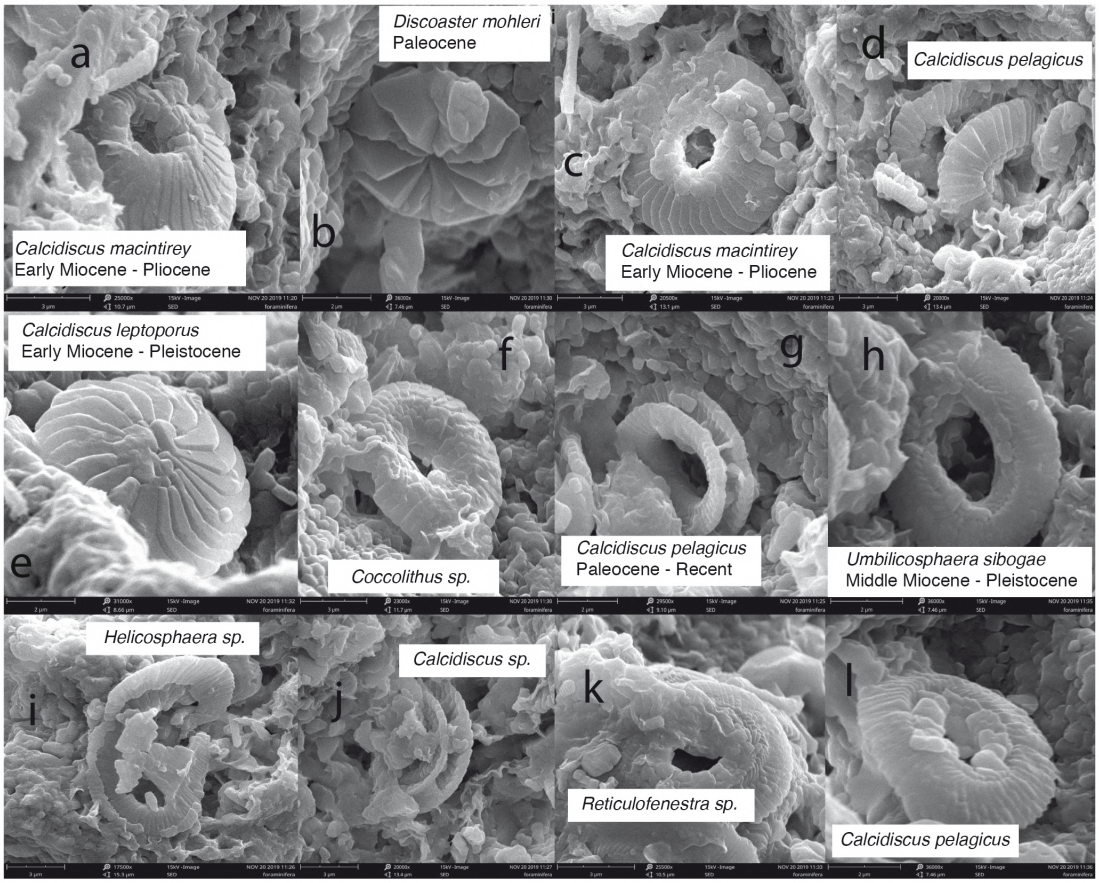

Figure 6. Calcareous nannofossil assemblages. *Analysed from the lowermost bedded chalky limestone.*

4.2 Reef Morphology

The reefal limestones of the Kalianga Formation mostly appear in North Sumba; they were formed as carbonate series and were uplifted to form sequences of coral reef terraces, representing major geomorphic features along the coast (Figure 2a; Effendi & Apandi, 1993; Satyana & Purwaningsih, 2011b; Nexer et al., 2015; Chauveau et al., 2021a; Authemayou et al., 2022; Chauveau et al., 2022). In Tambolaka and the surrounding area, we identified seven reef terraces in the field and from the DEM data (Figure 2b) and correlate them to the well-described sequence of Eastern Sumba (Figure 7). The lower terrace is developed at an elevation of ~8-10 m, is up to 200 m wide and stretches along the coast of NW-Sumba forming steep rocky cliffs. The second terrace is developed at a height of ~18-20 m with a width of at least 400 m. Based on our lateral correlation of terraces (Figure 7), we propose this terrace is the equivalent of terrace II_1 (± 60 m high; MIS 5e) at Cape Laundi (Pirazzoli et al., 1993, 1991; Chauveau et al., 2022). The third terrace developed at an elevation of ~28-34 m high and is at least 1 km wide. We propose that this terrace corresponds to terrace II_5 (± 105 m high; MIS 7e) at Cape Laundi (Figure 7; Pirazzoli et al., 1993, 1991; Chauveau et al., 2022). The fourth terrace is a relatively narrow terrace of a few hundred m wide, at an elevation of ~43-46 m. The fifth terrace has a width of ~1 km and is at an elevation of ~50-57 m. We propose that this terrace corresponds to Reef III (± 165 m high; MIS 9e) at Cape Laundi (Figure 7; Pirazzoli et al., 1993, 1991; Chauveau et al., 2022). The sixth terrace has a width of ~1.5 km and lies at an elevation of ~57-60 m. The seventh terrace has a width of ~500 m and lies at an elevation of ~68-72 m. We propose that this terrace corresponds to the distal

edge of Reef IV (± 210-230 m high; MIS 11c) at Cape Laundi (Figure 7; Pirazzoli et al., 1993, 1991; Chauveau et al., 2022). From diving observations, we found a ~75 m wide reef with living corals at ~2 m depth, and a second ~75 m wide reef at ~6 m depth.

Reef terrace	Elevation (m)	Width (m)	Lateral correlation at Cape Laundi		
			Elevation (m)	Terraces	Age
T1	8-10	~ 200	-	-	-
T2	18-20	~ 400	60	II_1	MIS 5e
T3	28-34	~1000	105	II_5	MIS 7e
T4	43-46	>100	-	-	-
T5	50-57	~ 1000	165	III	MIS 9e
T6	57-60	~ 1500	-	-	-
T7	68-72	~ 500	210-230	IV	MIS 11c

Table 1. Summary of onshore reef terrace at Tambolaka. *Assessed as lateral correlation with reef terraces at Cape Laundi NE-Sumba (Pirazzoli et al, 1991, 1993)*

Considering the lateral variations of the mapped reefs (Figure 7), there are clear trends that appear to be similar for Reefs II_1, II_5, III, and IV. Their elevations are relatively high to the SE of Cape Laundi and gradually decrease NW-wards, except for the area just W of Cape Laundi where elevations increase for ~4 km (Figure 7c). Then elevations decrease by almost half over ~30 km to Cape Sasar and again decrease by almost half for the ~50 km W of Cape Sasar. For the 50 km of coastal stretch around Tambolaka (Figure 7a, 7b), elevations of the terraces are approximately similar. Whereas Reefs II_5 and IV are relatively continuous and well-developed, Reefs II_1 and III are not always clear in morphology.

The mine pit is at ~2.5 km from the coastline, ~2 km E of the cross-section of Figure 2d. Assuming a sub-horizontal contact between the Wiakabukak and Kalianga Formations (at ~30 masl), we estimate that the open-cut pit would laterally be located below T5, T6, or T7 (Figure 2b). This implies a total thickness of ~20-40 m of Quaternary reefal limestones, which we used as a constraint for reef modeling (next section).

The present-day reef width varies in width between ~100 and ~500 m (Figure 8a), but generally, reefs are a little wider towards Cape Laundi than near Tambolaka. The total reefal terrace width offshore varies more dramatically between Tambolaka and Cape Laundi (Figure 8a), from around 1 km width for the ~100 km W of Cape Sasar but increasing towards ~5 km width at Cape Laundi. The offshore slopes (Figure 8b) are generally higher around Tambolaka, at around 10-25%, whereas they generally decrease E-ward to around 5% at Cape Laundi. Whereas slopes between 130-200 m depth and 130-400 m depth are roughly the same for the coastal stretch SE of Cape Sasar, for the coast W of Cape Sasar the 130-400 m slopes are consistently lower, indicating an overall

concave offshore slope. Overall, there is an apparent correlation between the width of the offshore reefal platform and the submarine slope of the island, but also with the apparent uplift rate, as indicated by the elevation of the fossil reefs (Figure 8). However, the width of the active reef is seemingly independent of these variables.

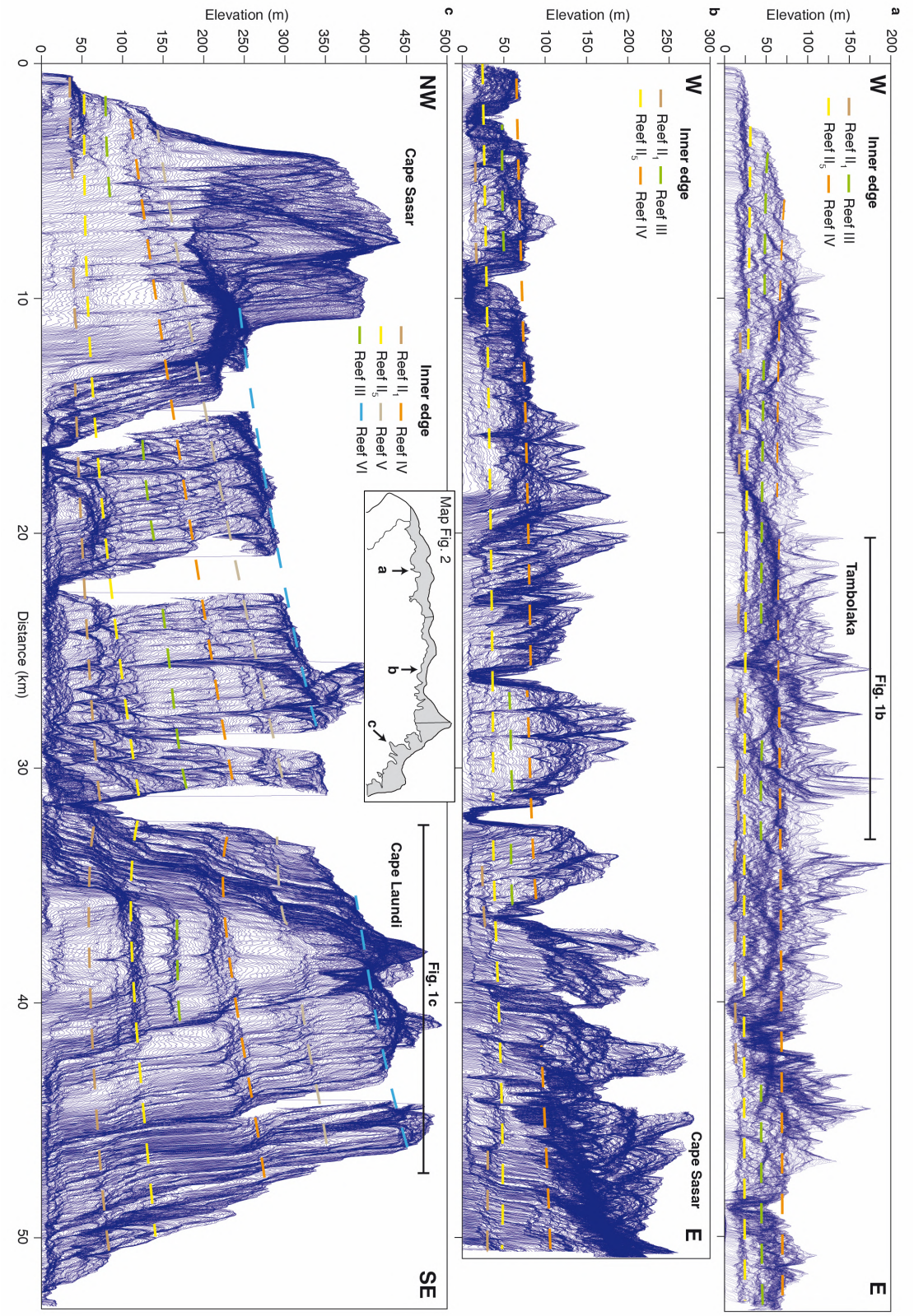

Figure 7 (Previous page). Stacked swath profiles of the NW Sumba coastline. *Figure shows a comparison of the coral reef terrace elevations for the area between Tambolaka and Cape Laundi in NW to NE-Sumba. Areas and viewing directions are given in Figure 2. The elevation shows a significant difference among the four mapped reef terraces with reef elevations decreasing by around 65-75% between Cape Laundi and Tambolaka.*

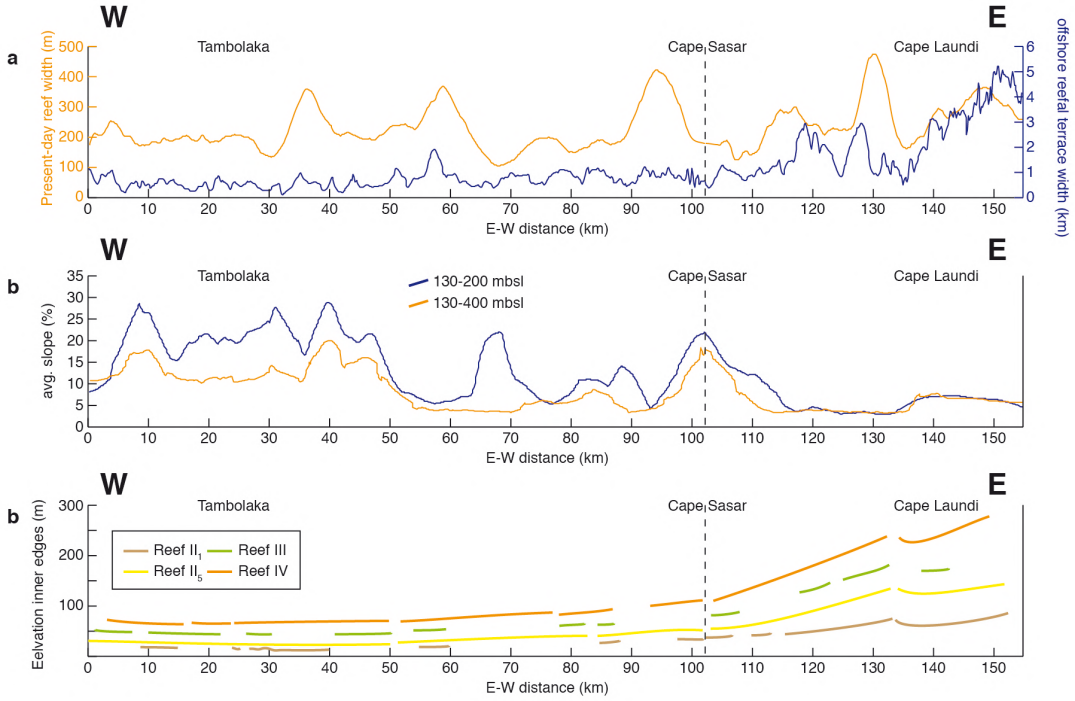

Figure 8. Lateral comparison of NW Sumba Coastline*. Comparison of several geomorphic reef terrace features between Cape Laundi and Tambolaka* ***(a)*** *Present-day reef width as mapped from Google Earth, and offshore reefal terrace width as approximated from the bathymetry (see Materials and Methods)* ***(b)*** *Average offshore slopes for depths of 130 to 200 m and 130 to 400 m* ***(c)*** *Reef terrace elevations for the 4 main reef terraces that were mapped in the stacked swath profiles of Figure 7.*

4.3 Reef Modeling

We use our modeling results to evaluate the reef morphology and geometry both quantitatively and qualitatively. By exploring the parametric fields, we can infer the conditions upon which the observed sequence has been developed. An important metric that our stratigraphic and microfossil analysis provided, which can be directly compared to the reef models, is the full thickness of Quaternary reefs above the mine pit. To achieve Quaternary reef thicknesses of 20-40 m (Figure 9b; see previous section) above elevations of 30 masl, potential reef growth rates have to be 2 mm/yr or less, irrespective of the modeled uplift rates, erosion rates, initial slopes and sea-level curves (Figure 10). The ensemble of modeling results demonstrates that the potential reef growth rate exerts a primary control on the total Quaternary reef thickness, especially for reef growth rates <4 mm/yr. For higher rates, the relation between total reef thickness and reef growth is less predictable, and higher potential reef growth rates do not necessarily imply a thicker total reef thickness. Uplift rates of 0.125 mm/yr

generally imply a thicker reef thickness than rates of 0.15 and 0.175 mm/yr, whereas the influence of erosion rate on reef thickness is not very obvious (Figure 10). Although we did not quantify reef thicknesses for the different initial slopes, the examples in Figure 9b show that changing the slope from 2% to 1% mostly changes the reef terrace width, but not the thickness.

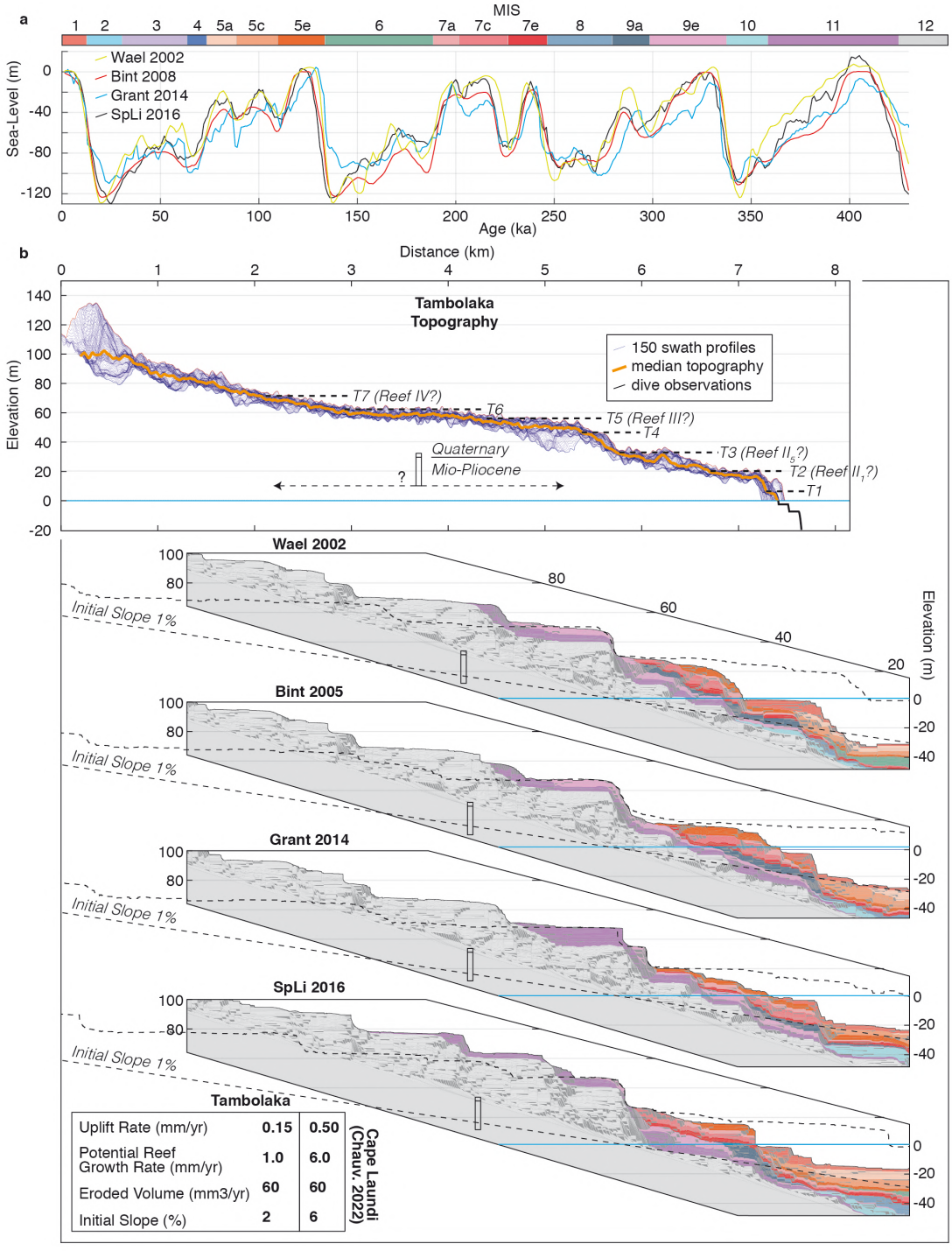

Figure 9. Modeling results for the Tambolaka sequence (a) *Sea-level curves tested with the model color codes referring to Marine Isotope Stages (MIS). Wael 2002 = Waelbroeck et al. (2002), Bint 2005 = Bintanja et al. (2005), Grant 2014 = Grant et al. (2014) and SpLi 2016 = Spratt and Lisiecki (2016)* ***(b)*** *Topography of the Tambolaka terrace sequence (same as Figure 2d) for comparison with the models. Models show the full reef architecture for initial*

slopes of 2%, and dotted lines show the topography and reef base for models with initial slopes of 1%. Model parameters are given in the left bottom inset and compared to the preferred model parameter values for Cape Laundi in Chauveau et al. (2022). Additional model examples are shown in Supplementary Figure 1.

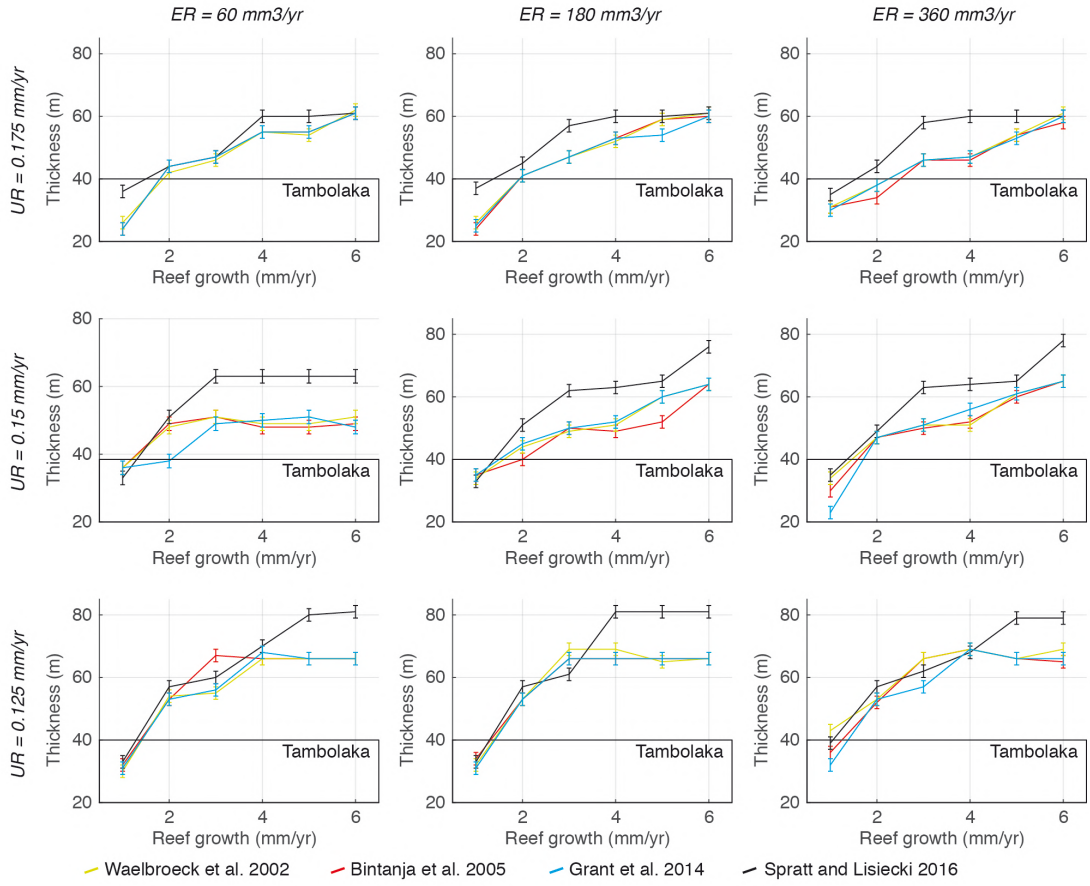

Figure 10. Modeled reef thicknesses for different parameters. *The stratigraphic and morphologic analysis suggests the full reef thickness at Tambolaka above an elevation of 30 m asl is ~20-40 m, only compatible with potential reef growth rates of 1-2 mm/yr. We tested different Uplift Rates (UR), Eroded Volumes (ER), and the four sea-level curves given in Figure 9a.*

Looking at the overall shape of the terrace sequences, the lower part of the sequence from T3 downwards is more consistent with an initial slope of 2%, and the part of the sequence above T3 with wider terraces is more consistent with an initial slope of 1% (dashed lines in Figure 9b). The limited width of the present-day reef that we observed offshore, consistently wider in the models, suggests a higher initial slope percentage offshore. This apparent convex morphology is the opposite of the apparent concave morphology offshore Tambolaka (see previous section). Taking the overall shape of the terrace sequence, all sea-level curves produce a relatively prominent cliff at the inner edge of the MIS 7e terrace, which is consistent with the observed profile and our age interpretation of the Tambolaka terraces. Elevations for this terrace vary per sea-level curve, but at elevations of ~20-30 m, they are comparable to the observed T3. In none of the models, there is a big cliff separating MIS 5 and MIS 7 reefs, which is also consistent with the observed profile, where the transition between T2 and T3 is defined by a gentle slope over an elevation change of ~5 m. All of the models show multiple MIS 5e terraces, of which some are at elevations of ~8-12 m like

the observed T1. Above the MIS 7 terrace, the models show 3 to 4 terraces between 40 and 80 m elevation, comparable to the observed T4-T7 terraces in the topography. For this section, the modeled morphology using the Spratt and Lisiecki (2016) curve with a 1% slope matches the observed morphology best: the elevations and locations of the three MIS 9-11 terraces are very similar to the T5, T6, and T7 terraces in the Tambolaka sequence. Offshore, the morphology modeled with the Bintanja et al. (2005) and Grant et al. (2014) curves is most similar to the observed two shallow and narrow terraces, showing how two Holocene terraces may have been created during one transgression. In a general sense, it seems terrace elevations are mostly controlled by sea-level highstands: all the modeled terrace surfaces have ages of either MIS 5, 7, 9, or 11. The width of the terraces seems to rely on the sea-level history of the preceding few hundred thousand years, as all modeled terraces were formed over multiple glacial-interglacial cycles given these slow uplift rates.

Supplementary Figure 1 shows some additional models with different parameters. Changing the erosion rate does not really affect the elevation of the reef terraces, nor the reef thickness, but it does change the width of some terraces. The uplift rate does change the elevations and morphology of the terrace sequence (Supplementary Figure 1). We note that generally, a 0.15 mm/yr uplift rate leads to terrace elevations that are more similar to the Tambolaka profile, with the exception of the models with the Grant et al. (2014) curve. In that curve, the MIS 9 and MIS 11 highstands are several meters lower than in the other curves, which may explain why a 0.175 mm/yr uplift rate leads to a better match with the observed terraces. Overall, our modeling results demonstrate that uplift rates, initial slopes, and potential reef growth rates at the Tambolaka sequence are all (much) lower than for the Cape Laundi sequence (inset Figure 9b).

5. DISCUSSION

5.1 Stratigraphic Correlation

A lithostratigraphic summary of a measured section of the Tambolaka mine pit reveals at least five different reef assemblages. In characteristics, there are considerable distinctions between the four lower layers and the uppermost layer, with the lower units consisting of a bedded chalky limestone unit with a moderately weakly cemented sandy matrix and the top unit consisting of a calcretized reefal limestone with a well-lithified sandy matrix (see Figure 3). The reef framework and facies descriptors are also somewhat different showing matrix-supported floatstone for the four lower layers and grain-supported rudstone for the uppermost layer. In addition, the domal coral-dominated (faviidae and poritidae) units identified in the four lower layers (see Figure 4) indicate deeper water environments either below the wave base or in protected areas of the back reef and the lagoon (Wood, 2011). While, in a wide-ranging core study of Indo-Pacific reefs (Montaggioni, 2005), domal coral occupies moderate energy environments in the form of a patch or bank barrier and shallow upward facies.

Based on planktonic foraminifera and nannofossil analyses, the relative age of the reef section in the Tambolaka mine pit confirms earlier observations from a Middle-Late Miocene section in W-Sumba (Abdullah et al., 2000). The important species for Late Miocene age in Tambolaka mine pit are *Globorotalia plesiotumida* and *Globorotalia tumida.* However, the lowermost bedded chalky limestone discovered the Oligocene species of *Globorotalia opima-opima.* We suppose that the Oligocene age of the lowermost section in the Tambolaka mine

pit has too wide a range due to the Oligocene period characterized by volcanic sediments (Abdullah et al., 2000). Nannofossil analysis was performed to evaluate the age of the lowermost bedded chalky limestone. The most important species is *Umbilicosphaera sibogae* discovered in the lowermost section. The species has the age Middle Miocene to Pleistocene (Bolli et al., 1985). Therefore, combined results of planktonic foraminifera and nannofossil analysis reveal that the age of the Tambolaka mine pit is mostly Middle to Late Miocene and is similar to the section in Lamboya Mountain and Jawila Mountain (Fig 1; Abdullah et al., 2000). The Quaternary portion of the mine pit section is relatively small, implying that the overall Quaternary thickness around Tambolaka does not exceed 20-40 m.

The carbonate series on Tambolaka in NW-Sumba conforms reasonably well to the Upper Miocene sediment and structure on Central Sumba (Waikabukak Formation; Fig. 1), constituting a bedded chalky limestone unit and pelagic marl (Abdullah et al., 2000). Nevertheless, they contrast with the turbiditic greywacke, tuff, and marly sandstone of Cape Laundi in NE-Sumba. The stratigraphic correlation between W and E-Sumba is marked by the interfingering structure between the carbonate series on W-Sumba and turbiditic sediments on E-Sumba, suggesting that the island tilted eastward during the Miocene (Satyana & Purwaningsih, 2011b; Fortuin et al., 1994, 1997). This observation is explained by the regional geodynamic framework. It is in accord with Fortuin et al. (1994, 1997) who postulated that the Sumba ridge was affected by eastward-increasing subsidence during the Lower Miocene. Overlying the Mio-Pliocene carbonate series on W-Sumba and Mio-Pliocene turbiditic sediments on E-Sumba, the Quaternary reefal limestones of the Kalianga Formation (Fig. 1) are well-preserved on both Tambolaka in NW-Sumba (Nexer et al., 2015; Authemayou et al., 2022) and Cape Laundi in NE-Sumba (Jouannic et al., 1988; Pirazzoli et al., 1991, 1993; Hantoro, 1992; Bard et al., 1996; Rutherford, 2001). The collision of the Australian continental plate in the eastern part of the Sunda-Banda islands arc around ~6 Ma (Haig, 2012) has resulted in a bulldozing effect in the crust of the island arc (Harris et al., 1992), and fast uplift of Sumba. The reefs have been uplifted, resulting in reef terraces along approximately two-thirds of the north, west, and east coast of the island (Hantoro, 1992; Fleury et al., 2009; Nexer et al., 2015). Hence, uplift of the Sumba ridge induced by the collision between the Australian plate margin and the Banda arc seems to be relatively young compared to the regional uplift of the outer arc of the Banda Islands (Hall & Smyth, 2008; Audley-Charles, 2011). This is also in line with Roep and Fortuin (1996), Harris (2011), and Pirazzoli et al., (1991, 1993) who demonstrated that the beginning of the uplifting process of Sumba ridge was at ~3 Ma in the east and ~1 Ma at Cape Laundi. This fast and recent uplift episode is due to tectonic shortening that adds up to the more regional, dynamic uplift of the entire Wallacea caused by the fast reorganization of the underlying subduction dynamics triggered by the collision of the Australian continent (Husson el al., 2022). In addition, Sumba is in the transition between the oceanic subduction and the continental subduction/collision (Fig. 1), and the temporal variation of uplift onset age compared with Banda islands is also due to this geodynamic pattern (Authemayou et al., 2022).

5.2 Reef Morphology and Modeling

U-series dating of raised coral reefs at Cape Laundi NE-Sumba (Pirazzoli et al., 1991, 1993; Bard et al., 1996) show that reef terraces along the north coast of Sumba have risen up to ± 450 m above sea level at a rate of 0.5-0.65 mm/yr since interglacial high sea levels. This effect is even more dramatic to the east (Timor), which rises up to ± 1700 m above sea level. The dating of a reef cap at 600 m above sea level on nearby Alor (Hantoro et al., 1994) indicates an uplift of

1.0-1.2 mm/yr. Thus, the uplift of that region is, at least locally, twice as fast as in E-Sumba.

Hantoro et al. (1995) demonstrated that E-Sumba experienced more rapid uplift rates (± 0.49 mm/yr) than the uplift rate on W-Sumba. Nexer et al. (2015) similarly showed that the uplift rates on the E-Sumba are considerably higher than those on W-Sumba, at 0.3-0.6 mm/yr and <0.3 mm/yr, respectively. Our estimate of ~0.15-0.2 mm/yr for Tambolaka, based on a detailed lateral correlation, is compatible with that. Going in more detail, our lateral terrace correlation refines earlier interpretations. The correlation by Nexer et al. (2015) of Reef IV (MIS 11) from Cape Laundi is similar to ours in overall trend, but suggests it corresponds to T5 in Tambolaka, and not T7 as we propose. Authemayou et al. (2022) proposed a stronger decrease in elevation of Reef IV terrace from Cape Laundi W-ward, correlating with T1 or T2 around Tambolaka. We attribute more confidence to our interpretation, as our analysis takes advantage of an 8 m-resolution DEM, from which we extracted swath profiles.

We show that the Cape Laundi coral reef terraces that are assigned to the last four major interglacial highstands (MIS 5e, 7e, 9e and 11c) can be correlated westwards, with their relative elevation differences remaining similar throughout the whole section (Figs. 7, 8). This suggests that Quaternary uplift has varied in space, but was approximately constant in time over the past ~400 ka. Apart from the laterally variable uplift rate, the coastal landform is notably different between the two sites, consisting of steep rocky cliff reefal limestone in Tambolaka and gently sloping beach (0-2%) of coarse organic sand with scattered corals in Cape Laundi. Furthermore, the present-day reef platform that corresponds to terrace 0 is submerged at Tambolaka but is exposed at Cape Laundi, where it is about 75-100 m wide and attains a width of 150-200 m in some particular areas (Pirazzoli et al., 1993; Chauveau et al., 2021a). Another interesting difference between NE and NW Sumba is the variability and difference in slopes. The Tambolaka section onshore suggests a convex morphology with initial slopes of 1-2% between -20 to 100 m elevation (Figure 9), whereas the offshore bathymetry suggests a concave morphology with slopes of 10-25% between -130 and -400 m elevation (Figure 8). In contrast, the on- and offshore bathymetry in Cape Laundi is surprisingly constant at ~6% on- and off-shore (Figs. 8, 9). We propose that this is directly related to the structural setting of N-Sumba, as Tambolaka is at the margin of the Sumba Ridge where slopes get steeper towards the NE-Lombok Basin northwards (Fig. 1) and then flatten again towards the basin center, and Cape Laundi is located more centrally on the ridge.

A key difference highlighted by the modeling based on the mine-pit section is the change in potential reef growth rate between Tambolaka and Cape Laundi, by a factor of 3 to 6. This emphasizes the importance of local oceanographic conditions on reef growth, even over distances of ~100 km, and can serve as a warning to reef modeling studies elsewhere. Generally speaking, many first order features can be well-reproduced in reef models of Cape Laundi (Chauveau et al., 2022) and Tambolaka (this study). To take a next step in uncovering further details on uplift and relative sea-level changes in Sumba, we suggest that future reef modelling work may include the addition of more terrace profiles in the region, as well as a probabilistic assesment of the model parameters.

Following the lines of Pastier et al. (2019) and Chauveau et al. (2022), our results show that the most prominent highstands do not necessarily produce the most prominent coral reef terraces. For example, in the modeled Tambolaka section the MIS 7e terrace seems to be persistently better developed than the MIS 5e terrace, even though the latter highstand was higher and lasted longer (Figure 9). In the models, the MIS 7e and 5e terraces grow on top of older reef platforms that started to affect the morphology well before 400 ka (Figure 9), showing how preceding sea-level and tectonic history will largely determine the accomodation

space available for reefs to grow. Another important demonstration, is that similar to Chauveau et al. (2022), also here our models show that one highstand can lead to several terraces (Figure 9), even if the highstand itself does not consist of several peaks (MIS 5 and 11 here for example). As such these models promote caution in linking coral reef terraces to sea-level highstands with a bijective approach (e.g. discussion in Dumas et al., 2006 and Hearty et al., 2007). A 'dynamic approach' (Pastier et al., 2019) like in this study is a way to allow for a more elaborate consideration of coral reef terrace chronology, which can be strengthened by analysing different terrace profiles simultaneously, and incorporating stratigraphic and geologic findings like we have demonstrated here.

6. CONCLUSIONS

We carried out a reef transect within the Tambolaka mine pit in NW-Sumba, which shows a bedded chalky limestone unit that contrasts with the turbiditic greywacke, tuff, and marly sandstone of Cape Laundi in NE-Sumba, suggesting different sedimentary environments during the Miocene. Planktonic foraminifera and calcareous nannofossils found in the Tambolaka mine pit indicate a wide range of ages between the Oligocene and Pliocene, and supports previously proposed E-ward tilting of N-Sumba during the Miocene.

Based on morphological observations and reef modeling we show that, compared to Cape Laundi, Tambolaka has a lower Quaternary uplift rate (~0.15-0.175 mm/yr instead of ~0.5 mm/yr), narrower present-day reef, lower slopes onshore, higher slopes offshore, and a much lower potential reef growth rate (~1-2 mm/yr instead of ~6 mm/yr). Based on lateral correlation with stacked swath profiles, and supported by reef modeling, we propose a new chronology for the coral reef terraces in NW-Sumba, with 7 terraces up to ~70 m elevation spanning the past ~400 ka. Our models show how the most prominent highstand does not necessarily produce the most prominent coral reef terrace, and it is mostly the preceding sea-level and tectonic history that will determine the accommodation space available for reefs to grow. This new analysis provides a better understanding of reef stratigraphy and morphodynamics of coral reef sequences, which may serve as a basis to further explore the relative sea-level and tectonic history of the island, as well as provide an example for paleo sea-level and coral reef terrace studies elsewhere.

ACKNOWLEDGEMENTS

We thank Kevin Pedoja and Anne-Morwenn Pastier for discussions and advice. SYC acknowledges the Program Insentif Riset Sistem Inovasi Nasional research grant to SYC number 071/ P/RPL-LIPI /INSINAS-I/II/I 2019, National Geographic Explore Grant to SYC number CP 087R 17 for Sumba fieldwork, Nusantara Research Grant to RR number 341/E4.1/AK.04.PT/2021, and to Alexander von Humboldt Digital Cooperation fellowship program to SYC. GDG acknowledges research permit 52/SIP/IV/FR/6/2022 provided by the Indonesian government on June 8th 2022. GDG acknowledges postdoctoral funding from the IRD and the Manajemen Talenta BRIN fellowship program 2022.

AUTHOR CONTRIBUTIONS

All authors have an equal main contribution. (a) conceptualization: TS, GDG, LH, SYC (b) funding acquisition: SYC (c) methodology: TS, GDG, DAU, MH, DC (d) investigation: TS, GDG, DAU, MH, RR, CA (g) supervision: LH, SYC (h) writing –

initial draft: TS, GDG, (i) writing – reviewing and editing: TS, GDG, DAU, MH, RR, DC, CA, LH, SYC

DATA AVAILABILITY STATEMENT

The topographic and bathymetric data used in this study is available for free at http://tides.big.go.id/DEMNAS and https://tanahair.indonesia.go.id/demnas/#/batnas. The coral reef terrace modeling code is available at https://github.com/Anne-Morwenn/REEF.

REFERENCES

Abdullah, C. ., Rampnoux, J.-P., Bellon, H., Maury, R., & Soeria-Atmadja, R. (2000). The evolution of Sumba Island (Indonesia) revisited in the light of new data on the geochronology and geochemistry of the magmatic rocks. *Journal of Asian Earth Sciences*, *18*(5), 533–546. https://doi.org/10.1016/S1367-9120(99)00082-6.

Armijo, R., Lacassin, R., Coudurier-Curveur, A., & Carrizo, D. (2015). Coupled tectonic evolution of Andean orogeny and global climate. *Earth-Science Reviews*, *143*, 1-35.

Audley-Charles, M. G. (1975). The Sumba fracture: A major discontinuity between eastern and western Indonesia. *Tectonophysics*, *26*(3–4), 213–228. https://doi.org/10.1016/0040-1951(75)90091-8

Audley-Charles, M.G. (2011). Tectonic post-collision processes in Timor. Geol. Soc. Lond., Spec. Publ. 355, 241–266. http://dx.doi.org/10.1144/SP355.12.

Authemayou, C., Brocard, G., Delcaillau, B., Molliex, S., Pedoja, K., Husson, L., ... & Cahyarini, S. Y. (2018). Unraveling the roles of asymmetric uplift, normal faulting and groundwater flow to drainage rearrangement in an emerging karstic landscape. *Earth Surface Processes and Landforms*, *43*(9), 1885-1898.

Authemayou, C., Pedoja, K., Chauveau, D., Husson, L., Brocard, G., Delcaillau, B., & Scholz, D. (2022). Deformation and uplift at the transition from oceanic to continental subduction, Sumba Island, Indonesia. *Journal of Asian Earth Sciences*, *236*, 105316.

Bard, E., Jouannic, C., Hamelin, B., Pirazzoli, P., Arnold, M., Faure, G., Sumosusastro, P., & Syaefudin. (1996). Pleistocene sea levels and tectonic uplift based on dating of corals from Sumba Island, Indonesia. *Geophysical Research Letters*, *23*(12), 1473–1476. https://doi.org/10.1029/96GL01279

Bintanja, R., Van De Wal, R. S., & Oerlemans, J. (2005). Modelled atmospheric temperatures and global sea levels over the past million years. *Nature*, *437*(7055), 125-128.

Bock, Y., Prawirodirdjo, L., Genrich, J.F., Stevens, C.W., McCaffrey, R., Subarya, C., Puntodewo, S.S.O., Calais, E., 2003. Crustal motion in Indonesia from Global Positioning System measurements. Geophys. Res. Lett. 108, 2367. https://doi.org/ 10.1029/2001JB000324, B8.

Bolli, H. M., Saunders, J. B., & Perch-Nielsen, K. (1985). *Plankton Stratigraphy Volume 1. Planktic foraminifera, calcareous nannofssils, and calpionellids*. Cambridge University Press.

Burollet, P., & Salle, C. (1981). A Contribution to the geological study of Sumba (Indonesia). *Proceedings Indonesian Petroleum Association. 10th Annual Convention*, 331–344.

Camoin, G. F., & Webster, J. M. (2015). Coral reef response to Quaternary sea-level and environmental changes: State of the science. *Sedimentology*, *62*(2), 401–428. https://doi.org/10.1111/sed.12184

Chappell, J. (1974). Geology of coral terraces, Huon Peninsula, New Guinea: a study of Quaternary tectonic movements and sea-level changes. *Geological Society of America Bulletin*, *85*(4), 553-570.

Chappell, J. and H. Polach (1991).Post-glacial sea-level rise from a coral record at Huon Peninsula, Papua New Guinea. *Nature,* 349(6305): 147-149.

Chappell, J. (2002). Sea level changes forced ice breakouts in the Last Glacial cycle: new results from coral terraces. *Quaternary Science Reviews*, *21*(10), 1229-1240.

Chauveau, D., Authemayou, C., Pedoja, K., Molliex, S., Husson, L., Scholz, D., Godard, V., Pastier, A.-M., de Gelder, G., Cahyarini, S. Y., Elliot, M., Weber, M., Benedetti, L., Jaud, M., Boissier, A., Agusta, V. C., Aribowo, S., Budd, A. F., & Natawidjaja, D. H. (2021a). On the generation and degradation of emerged coral reef terrace sequences: First cosmogenic 36Cl analysis at Cape Laundi, Sumba Island (Indonesia). *Quaternary Science Reviews*, *269*, 107144. https://doi.org/10.1016/j.quascirev.2021.107144

Chauveau, D., Authemayou, C., Molliex, S., Godard, V., Benedetti, L., Pedoja, K., Husson, L., & Cahyarini, S. Y. (2021b). Eustatic knickpoint dynamics in an uplifting sequence of coral reef terraces, Sumba Island, Indonesia. *Geomorphology*, *393*, 107936. https://doi.org/10.1016/j.geomorph.2021.107936

Chauveau, Denovan; Rovere, Alessio (2022): Modeling coral reef terraces: The Last Interglacial at Cape Laundi (Sumba Island, Indonesia). figshare. Presentation. https://doi.org/10.6084/m9.figshare.20368224.v4

de Gelder, G., Jara-Muñoz, J., Melnick, D., Fernández-Blanco, D., Rouby, H., Pedoja, K., ... & Lacassin, R. (2020). How do sea-level curves influence modeled marine terrace sequences?. *Quaternary Science Reviews*, *229*, 106132.

de Gelder, G., Husson, L., Pastier, A. M., Fernández-Blanco, D., Pico, T., Chauveau, D., ... & Pedoja, K. (2022). High interstadial sea levels over the past 420ka from the Huon Peninsula, Papua New Guinea. *Communications Earth & Environment*, *3*(1), 1-12.

Dumas, B., Hoang, C. T., & Raffy, J. (2006). Record of MIS 5 sea-level highstands based on U/Th dated coral terraces of Haiti. *Quaternary International*, *145*, 106-118.

Effendi, A. & Apandi, C. (1993). *Geological map of Sumba quadrangle, Nusa Tenggara Sheet (1:250,000)*.

Embry, A. F., & Klovan, J. E. (1971). A Late Devonian reef tract on northeastern banks island, N.W.T.1. *Bulletin of Canadian Petroleum Geology*, *19*(4), 730–781. https://doi.org/https://doi.org/10.35767/gscpgbull.19.4.730

Fairbanks, R. G. (1989).A 17,000-year glacio-eustatic sea level record.influence of glacial melting rates on the Younger Dryas event and deep ocean circulation. *Nature*, 342, 637–642.

Fernández-Blanco, D., de Gelder, G., Lacassin, R., & Armijo, R. (2020). Geometry of flexural uplift by continental rifting in Corinth, Greece. *Tectonics*, *39*(1), e2019TC005685.

Fleury, J.-M., Pubellier, M., de Urreiztieta, M. (2009). Structural expression of forearc crust uplift due to subducting asperity. Lithos 113 (1), 318–330. http://dx.doi.org/10. 1016/j.lithos.2009.07.007.

Fortuin, A.R., Roep, T.B., Sumosusastro, P.A. (1994). The Neogene sediments of Eastern Sumba, Indonesia—products of a lost arc? J. SE Asian Earth Sci. 9 (1–2), 67–79.

Fortuin, A.R., Van derWerff,W.,Wensink, H. (1997). Neogene basin history and paleomagnetism of a rifted and inverted forearc region, on-and offshore Sumba, Eastern Indonesia. J. Asian Earth Sci. 15, 61–88. http://dx.doi.org/10.1016/S0743- 9547(96)00081-5.

Grant, K. M., Rohling, E. J., Ramsey, C. B., Cheng, H., Edwards, R. L., Florindo, F., & Williams, F. (2014). Sea-level variability over five glacial cycles. *Nature communications*, *5*(1), 1-9.

Haig, D.W. (2012). Palaeobathymetric gradients across Timor during 5.7–3.3 Ma (latest Miocene–Pliocene) and implications for collision uplift. Palaeogeogr. Palaeoclimatol. Palaeoecol. 331–332, 50–59. http://dx.doi.org/10.1016/j.palaeo.2012.02.032.

Hall, R., Smyth, H.R. (2008). Cenozoic arc processes in Indonesia: identification of the key influences on the stratigraphic record in active volcanic arcs, in: Special Paper 436: Formation and Applications of the Sedimentary Record in Arc Collision Zones. Geol. Soc. Am. 27–54.

Hamilton, W. (1979). *Tectonics of the Indonesia Region: Geological Survey Professional paper*.

Hantoro, W. (1992). Etude des terrasses récifales quaternaires soulevées entre le détroit de la Sonde et l'île de Timor, Indonésie. Mouvements Verticaux de la Croûte terrestre et variations du niveau de la mer, PhD Thesis Univ. d'Aix Marseille II, France.

Hantoro, W.S., Pirazzoli, P.A., Jouannic, C. H. Faure, C. T. Hoang, U. Radtke, C. Causse, M. Borel Best, R. Lafont, S. Bieda & K. Lambeck (1994). Quaternary uplifted coral reef terraces on Alor Island, East Indonesia. *Coral Reefs* **13**, 215–223. https://doi.org/10.1007/BF00303634.

Hantoro, W. S., Lafont, R., Bieda, S., Handayani, L., Sebowo, E., & Hadiwisastra, S. (1995). Holocene to recent vertical movement in Indonesia: Study on emerged coral reef. *Proceedings of the International Conference on Geology of South East Asia*, 93–113.

Harris, R. A. (1991). Temporal distribution of strain in the active Banda orogen: a reconciliation of rival hypotheses, in Orogenesis in Action, (eds. E. Hall, G. Nichols, and C. Rangin), Spec V. Journal of Asian Earth Sci., V.6, No. 3/4, p. 373-386.

Harris, R. A., Wu, S., & Charlton, T. R. (1992). Comment and Reply on "Postcollision extension in arc-continent collision zones, eastern Indonesia." *Geology*, *20*(1), 92. https://doi.org/10.1130/0091-7613(1992)020<0092:CAROPE>2.3.CO;2

Harris, R. (2011). The nature of the banda arc–continent collision in the timor region. Arc–Continent Collision, Frontiers in Earth Sciences. Springer Berlin

Heidelberg, pp. 163–211 http://dx.doi.org/10.1007/978-3-540-88558-0_7.

Hearty, P. J., Neumann, A. C., & O'Leary, M. J. (2007). Comment on "Record of MIS 5 sea-level highstands based on U/Th dated coral terraces of Haiti" by Dumas et al.[Quaternary International 2006 106–118]. *Quaternary international*, *162*, 205-208.

Husson, L., Pastier, A. M., Pedoja, K., Elliot, M., Paillard, D., Authemayou, C. & Cahyarini, S. Y. (2018). Reef carbonate productivity during quaternary sea level oscillations. *Geochemistry, Geophysics, Geosystems*, *19*(4), 1148-1164.

Jouannic, C., Hantoro, W. S., Hoang, C. T., Fournier, M., Lafont, R., & Ichram, M. L. (1988). Quaternary raised reef terraces at Cape Laundi, Sumba, Indonesia: geomorphological analysis and first radiometric (Th/U and 14C) age determinations. *Proceedings of the 6th International Coral Reef Symposium*, 441–447.

Montaggioni, L. F. (2005). History of Indo-Pacific coral reef systems since the last glaciation: Development patterns and controlling factors. *Earth-Science Reviews*, *71*(1–2), 1–75. https://doi.org/10.1016/j.earscirev.2005.01.002

Nexer, M., Authemayou, C., Schildgen, T., Hantoro, W. S., Molliex, S., Delcaillau, B., Pedoja, K., Husson, L., & Regard, V. (2015). Evaluation of morphometric proxies for uplift on sequences of coral reef terraces: A case study from Sumba Island (Indonesia). *Geomorphology*, *241*, 145–159. https://doi.org/10.1016/j.geomorph.2015.03.036

Nugroho, H., Harris, R., Lestariya, A.W., Maruf, B. (2009). Plate boundary reorganization in the active Banda Arc–continent collision: Insights from new GPS measurements. Tectonophysics 479 (1–2), 52–65.

Pacheco, J.F., Sykes, L.R., Scholz, C.H. (1993). Nature of seismic coupling along simple plate boundaries of the subduction type. J. Geophys. Res. Solid Earth 98 (B8), 14133–14159

Pastier, A. M., Husson, L., Pedoja, K., Bézos, A., Authemayou, C., Arias-Ruiz, C., & Cahyarini, S. Y. (2019). Genesis and architecture of sequences of Quaternary coral reef terraces: Insights from numerical models. *Geochemistry, Geophysics, Geosystems*, *20*(8), 4248-4272.

Peltier, W. R. and R. G. Fairbanks (2006).Global glacial ice volume and Last Glacial Maximum duration from an extended Barbados sea level record.*Quaternary Science Reviews,*25(23–24): 3322-3337.

Pirazzoli, P. A., Radtke, U., Hantoro, W. S., Jouannic, C., Hoang, C. T., Causse, C., & Best, M. B. (1991). Quaternary Raised Coral-Reef Terraces on Sumba Island, Indonesia. *Science*, *252*(5014), 1834–1836. https://doi.org/10.1126/science.252.5014.1834

Pirazzoli, P. A., Radtke, U., Hantoro, W. S., Jouannic, C., Hoang, C. T., Causse, C., & Best, M. B. (1993). A one million-year-long sequence of marine terraces on Sumba Island, Indonesia. *Marine Geology*, *109*(3–4), 221–236. https://doi.org/10.1016/0025-3227(93)90062-Z

Rangin, C., Jolivet, L., & Pubellier, M. A. N. U. E. L. (1990). A simple model for the tectonic evolution of southeast Asia and Indonesia region for the past 43 my. *Bulletin de la Soci´et´e g´eologique de France*, *6*(6), 889–905.

Roep, T.B., Fortuin, A.R. (1996). A submarine slide scar and channel filled with slide blocks and megarippled Globigerina sands of possible contourite

origin from the Pliocene of Sumba Indonesia. Sedim. Geol. 103 (1–2), 145–160.

Rutherford, E., Burke, K., Lytwyn, J. (2001). Tectonic history of Sumba Island, Indonesia, since the Late Cretaceous and its rapid escape into the forearc in the Miocene. J. Asian Earth Sci. 19 (4), 453–479. http://dx.doi.org/10.1016/S1367-9120(00)00032-8.

Satyana, A. H., & Purwaningsih, M. E. (2011a). Multidisciplinary approaches on the origin of Sumba Terrane: Regional geology, historical biogeography, linguistic-genetic coevolution and megalithic archeology. *36th HAGI and 40th IAGI Annual Convention and Exhibition*, 1–29.

Satyana, A. H., & Purwaningsih, M. E. (2011b). Sumba area: detached Sundaland terrane and petroleum implications. *Proceedings of Indonesian Petroleum Association, 35th Annual Convention*, 1–32.

Simons, W.J.F., Socquet, A., Vigny, C., Ambrosius, B.A.C., Haji Abu, S., Promthong, C., Spakman, W. (2007). A decade of GPS in Southeast Asia: Resolving Sundaland motion and boundaries. J. Geophys. Res. Solid Earth 112 (B6).

Soeria-Atmadja, R., Suparka, S., Abdullah, C., Noeradi, D., & Sutanto. (1998). Magmatism in western Indonesia, the trapping of the Sumba Block and the gateways to the east of Sundaland. *Journal of Asian Earth Sciences*, *16*(1), 1–12. https://doi.org/10.1016/S0743-9547(97)00050-0

Spakman, W., Hall, R. (2010). Surface deformation and slab–mantle interaction during Banda arc subduction rollback. Nat. Geosci. 3 (8), 562–566

Spratt, R. M., & Lisiecki, L. E. (2016). A Late Pleistocene sea level stack. *Climate of the Past*, *12*(4), 1079-1092.

Tate, G.W., McQuarrie, N., Van Hinsbergen, D.J.J., Bakker, R.R., Harris, R., Willett, S., et al. (2014). Resolving spatial heterogeneities in exhumation and surface uplift in Timor-Leste: constraints on deformation processes in young orogens. Tectonics 33 (6), 1089e1112

Taylor, F. W., & Mann, P. (1991). Late Quaternary folding of coral reef terraces, Barbados. *Geology*, *19*(2), 103-106.

Tomascik, T., Mah, A. J., Nontji, A., & Moosa, M. K. (1997). *The Ecology of the Indonesia Seas Volume VIII Part II*. Oxford University.

Waelbroeck, C., Labeyrie, L., Michel, E., Duplessy, J. C., Mcmanus, J. F., Lambeck, K., ... & Labracherie, M. (2002). Sea-level and deep water temperature changes derived from benthic foraminifera isotopic records. *Quaternary science reviews*, *21*(1-3), 295-305.

Wensink, H., van Bergen, M.J. (1995). The tectonic emplacement of Sumba in the Sunda- Banda Arc: paleomagnetic and geochemical evidence from the early Miocene Jawila volcanics. Tectonophysics 250 (1–3), 15–30.

Wood, R. (2011). General evolution of carbonate reefs in David Hopley (ed.), Encyclopedia of Modern Coral Reefs. DOI 10.1007/978-90-481-263

SUPPORTING INFORMATION

Supplementary Figure 1. Additional reef models (a) Models with variable eroded volumes (ER) and potential reef growth rates (RGR). The topmost model is the same as in Figure 9 for comparison. **(b)** Models with different uplift rates using the sea-level curves of Waelbroeck et al. (2002) and Bintanja et al. (2005). The models with 0.15 mm/yr are the same as in Figure 9 for comparison. **(c)** Models with different uplift rates using the sea-level curves of Grant et al. (2014) and Spratt and Lisiecki (2016). The models with 0.15 mm/yr are the same as in Figure 9 for comparison.

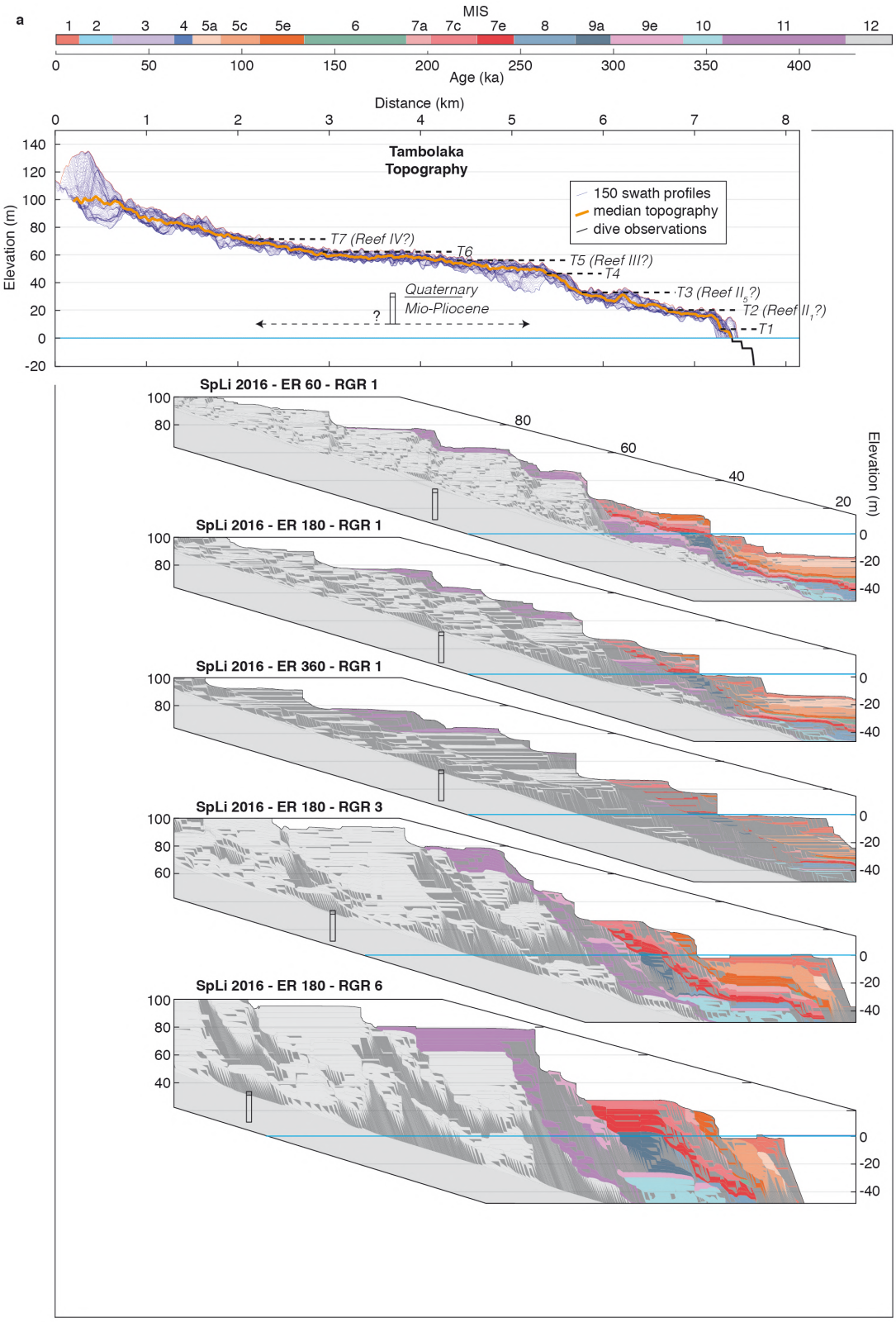
a
MIS
1 2 3 4 5a 5c 5e 6 7a 7c 7e 8 9a 9e 10 11 12
0 50 100 150 200 250 300 350 400
Age (ka)
Distance (km)
0 1 2 3 4 5 6 7 8
Tambolaka
Topography
150 swath profiles
median topography
dive observations
Elevation (m)
140 120 100 80 60 40 20 0 -20
T7 (Reef IV?)
T6
T5 (Reef III?)
T4
T3 (Reef II$_5$?)
T2 (Reef II$_1$?)
T1
Quaternary
Mio-Pliocene
?
SpLi 2016 - ER 60 - RGR 1
SpLi 2016 - ER 180 - RGR 1
SpLi 2016 - ER 360 - RGR 1
SpLi 2016 - ER 180 - RGR 3
SpLi 2016 - ER 180 - RGR 6
100 80 60 40 20
Elevation (m)
0 -20 -40

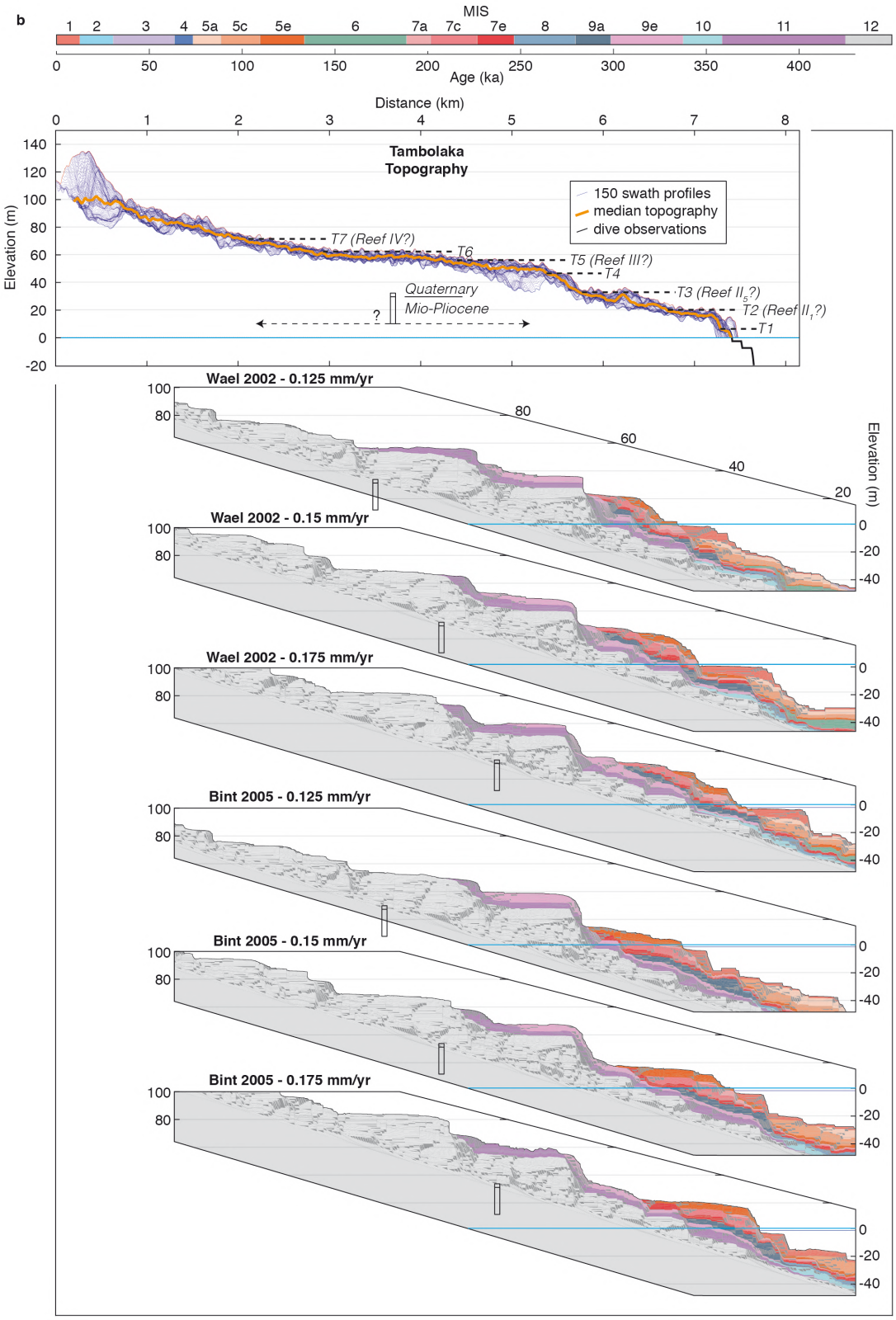
b
MIS
1 2 3 4 5a 5c 5e 6 7a 7c 7e 8 9a 9e 10 11 12
0 50 100 150 200 250 300 350 400
Age (ka)
Distance (km)
0 1 2 3 4 5 6 7 8
Tambolaka
Topography
150 swath profiles
median topography
dive observations
Elevation (m)
140 120 100 80 60 40 20 0 -20
T7 (Reef IV?)
T6
T5 (Reef III?)
T4
T3 (Reef II$_5$?)
T2 (Reef II$_1$?)
T1
Quaternary
Mio-Pliocene
?
Wael 2002 - 0.125 mm/yr
Wael 2002 - 0.15 mm/yr
Wael 2002 - 0.175 mm/yr
Bint 2005 - 0.125 mm/yr
Bint 2005 - 0.15 mm/yr
Bint 2005 - 0.175 mm/yr
100 80
80 60 40 20
Elevation (m)
0 -20 -40

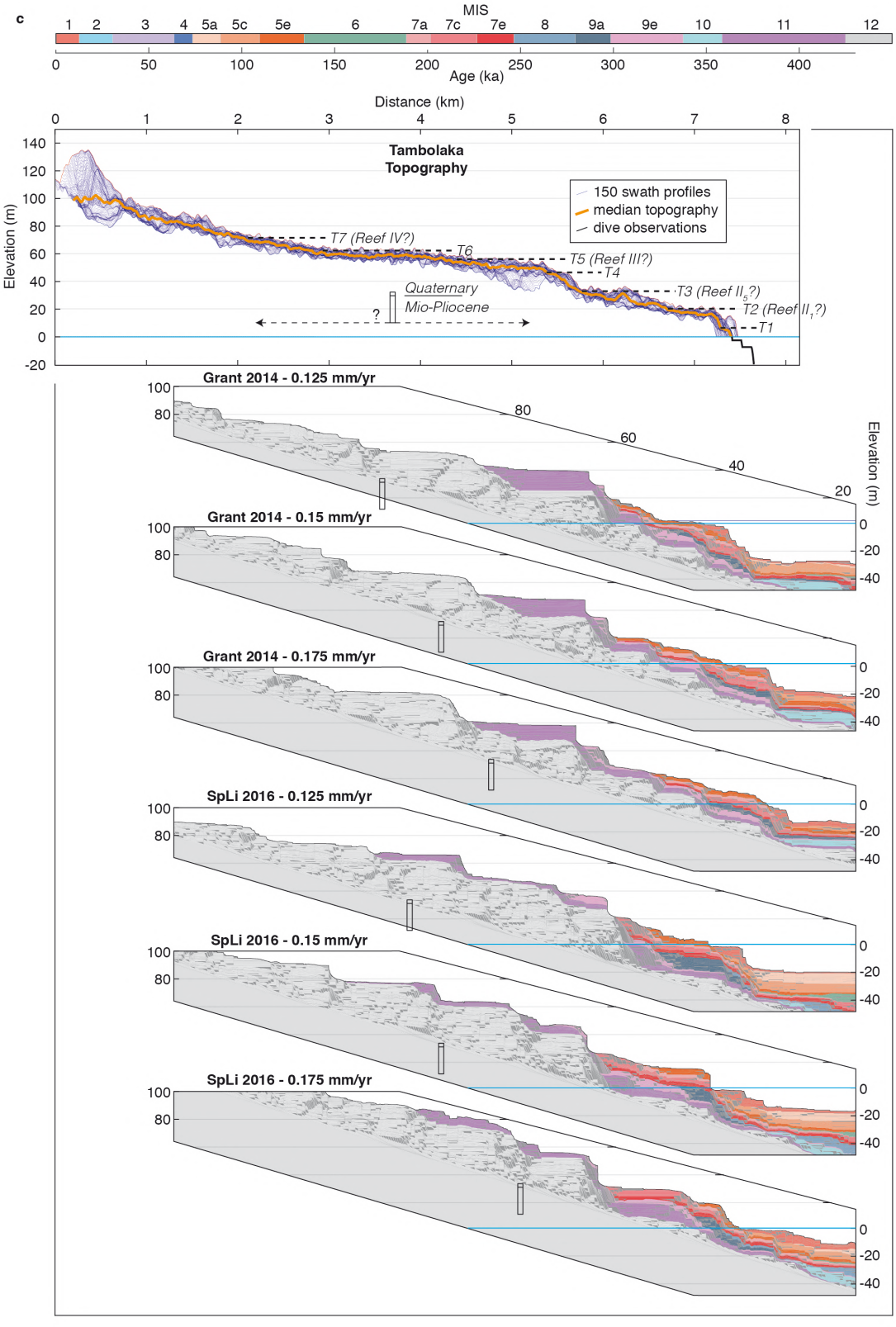
c
MIS
1 2 3 4 5a 5c 5e 6 7a 7c 7e 8 9a 9e 10 11 12
0 50 100 150 200 250 300 350 400
Age (ka)
Distance (km)
0 1 2 3 4 5 6 7 8
Elevation (m)
140 120 100 80 60 40 20 0 -20
Tambolaka
Topography
150 swath profiles
median topography
dive observations
T7 (Reef IV?)
T6
T5 (Reef III?)
T4
T3 (Reef II$_s$?)
T2 (Reef II$_1$?)
T1
Quaternary
Mio-Pliocene
?
Grant 2014 - 0.125 mm/yr
Grant 2014 - 0.15 mm/yr
Grant 2014 - 0.175 mm/yr
SpLi 2016 - 0.125 mm/yr
SpLi 2016 - 0.15 mm/yr
SpLi 2016 - 0.175 mm/yr
100 80
80 60 40 20
Elevation (m)
0 -20 -40